1992

Hypoid gear optimization

Selvaraj Ramachandran
Portland State University

AN ABSTRACT OF THE THESIS OF Selvaraj Ramachandran for the Master of Science in Mechanical Engineering presented February 11, 1992.

Title: Hypoid Gear Optimization.

APPROVED BY THE MEMBERS OF THE THESIS COMMITTEE:

[redacted]

[redacted]

[redacted]

A hypoid gear optimization procedure using the method of feasible directions has been developed. The objective is to reduce the gear set weight with bending strength, contact strength and facewidth-diametral pitch ratio as constraints. The objective function weight, is calculated from the geometric approximation of the volume of the gear and pinion. The design variables selected are number of gear teeth, diametral pitch, and facewidth. The input parameters for starting the initial design phase are power to be transmitted, speed, gear ratio, type of application, mounting condition, type of loading, and the material to be used. In the initial design phase, design parameters are selected or calculated using the standard available procedures. These selected values of design parameters are passed on to the optimization routine as starting points.

The design problem is first linearized to find the search direction. Along this search direction, the minimum value is found using the Golden section search method. The iterations are continued until the minimum value is reached or the constraints are violated. The final output

gives the optimized design variables and weight. To analyze the changes in design variables and objective function during each iteration, comparison tables and graphs are created.

HYPOID GEAR OPTIMIZATION

by
SELVARAJ RAMACHANDRAN

A thesis submitted in partial fulfillment of the
requirements for the degree of

MASTER OF SCIENCE
IN
MECHANICAL ENGINEERING

Portland State University
1992

TO THE OFFICE OF GRADUATE STUDIES:

The members of the committee approve the thesis of Selvaraj Ramachandran presented February 11, 1992.

[redacted]

Hormoz Zarefar, Chair

[redacted]

Faryar Etesami

[redacted]

George Lendaris

APPROVED:

[redacted]

Graig A. Spolek, Chair, Department of Mechanical Engineering

[redacted]

C. William Savery, Interim Vice Provost for Graduate Studies and Research

ACKNOWLEDGEMENTS

I record my sincere gratitude to all the people who has given their support, guidance, and timely advises that has helped me in the successful completion of this research work. My sincere appreciation to my advisor, Dr. Hormoz Zarefar for his enthusiasm, guidance and the care he showed on my academic and career development. I am very thankful to Dr. Faryar Etesami for providing his ideas and thoughts on the subject. I express my special thanks to Dr. Graig Spolek, Debbie, and Maxine for their attention and support.

All my effort will be fruitless without thanking the members of my family - my parents, my sister and my uncle Mr. Krishnamurty for their keenness shown in my studies and success. My dear friends Charles, Kishore, Mr. Edward Rickford, Rajkumar, Muthu and Jorge, all receive my appreciation and gratitude for making my stay in Portland, memorable and pleasant.

TABLE OF CONTENTS

LIST OF TABLES

TABLE PAGE

LIST OF FIGURES

CHAPTER I

INTRODUCTION

1.1 BACKGROUND

In the most general terms, optimization theory is a body of mathematical results and numerical methods for finding and identifying the best candidate from a collection of alternatives without having to explicitly enumerate and evaluate all possible alternatives [1]. The process of optimization lies at the root of engineering, since the classical function of the engineer is to design new, better, more efficient, and less expensive systems as well as to devise plans and procedures for the improved operation of existing systems.

Any problem in which certain parameters need to be determined to satisfy constraints can be formulated as an optimum design problem. Good problem formulation is the key to the success of an optimization study and is to a large degree an art. Optimization techniques are quite general, having a wide range of applications in diverse fields. The range of applications is limited only by the imagination or ingenuity of design engineers.

In engineering applications optimization criteria could be either economic factors or technological factors. The technological factors for instance, might be maximum torque, minimum weight, minimum energy utilization, maximum production rate, and so on. Regardless of the criterion selected, in the context of optimization the "best" will always mean the candidate system with either the minimum or maximum value of the performance index [1].

After selecting the performance criterion, the next key element is the selection of independent design variables that are adequate enough to characterize the design formulation. Once the variables are selected, the problem model has to be assembled in a manner that the performance criterion is influenced by the independent variables.

Optimization gives a systematic approach and insight to design decisions, where one relies heavily on intuition and experience. But this does not wholly mean that the design process can be reduced to a computer work and intuitive thinking is unimportant; rather it helps in automating the process and spending more time on the creative aspects.

Some of the initial optimization studies were conducted by necessity in order to mitigate inherently unavoidable dynamic stresses, forces, and vibrations to tolerable degrees in high speed mechanisms. Having been inspired by the results of these embryonic optimum design studies, one of the early pioneers in optimum design Ray C. Johnson [4], conducted many others for a broader range of bases for optimum design.

1.2 DESIGN PROCESS AND ROLE OF COMPUTERS

Mechanical design is one of the most challenging problems which can confront a practicing engineer. The complex relationships existing among the factors associated with the definition of design is the cause of such a challenge. Mechanical design can be defined as the selection of materials and geometry which satisfies specified and implied functional requirements while remaining within the confines of unavoidable limitations. The basic problem of design is considered more difficult than the problem of analysis, since for the latter, both geometry and materials are assumed to be known constants and limitations such as space restrictions are of no significance.

Design is an iterative process. The designer's experience, intuition, and ingenuity are required in the process of design. Iteration involves analyzing several trial systems in a sequence before an acceptable design is obtained. Such repetitive calculations are ideally suited for computer implementation.

Before computers, engineering designs were evaluated the hard way. They were built, tested, modified, retested, remodified - and so on. Computers improved the process dramatically, enabling much of the evaluation to be done with mathematical models rather than expensive prototyping. But that did not help the designer. The designer still had the root problem of juggling parameter values to find the right combination. And since there are endless possibilities, one could only hope that the final intuitive design was close to optimal.

The overall design process, shown in Figure 1, consists of an iterative cycle involving definition of the structure of the system, model formulation, model parameter optimization, and analysis of the resulting solution. The final optimal design will be obtained only after solving a series of optimization problems.

1.3 PROBLEM FORMULATION

In this topic, mathematical formulation of a design optimization problem is discussed. The problem is always converted to minimization of a cost function with proper constraints on design variables.

All machines and components are designed with an objective in mind. The objective can be weight, cost, life, efficiency, reliability or other merit measures, which are calculable functions of design variables. Similarly, there are usually a number of operational constraints placed on the design, such as stress limits, load limits, and size limits, which again are functions of the design variables.

The task of formulating the optimum design problem mainly hinges on proper identification of design variables. After identifying the proper variables, the cost and constraint functions should be formulated in terms of these variables.

It must be realized that the overall process of designing systems in different fields of engineering is roughly the same. Analytical and numerical methods for analyzing various systems can differ somewhat. Statement of the design problems can contain terminology that is specific to the particular domain of application. However, once the problem from different fields have been converted into mathematical statements using a standard notation, they all look alike [2].

The standard design optimization model is defined as follows: Find an n-vector

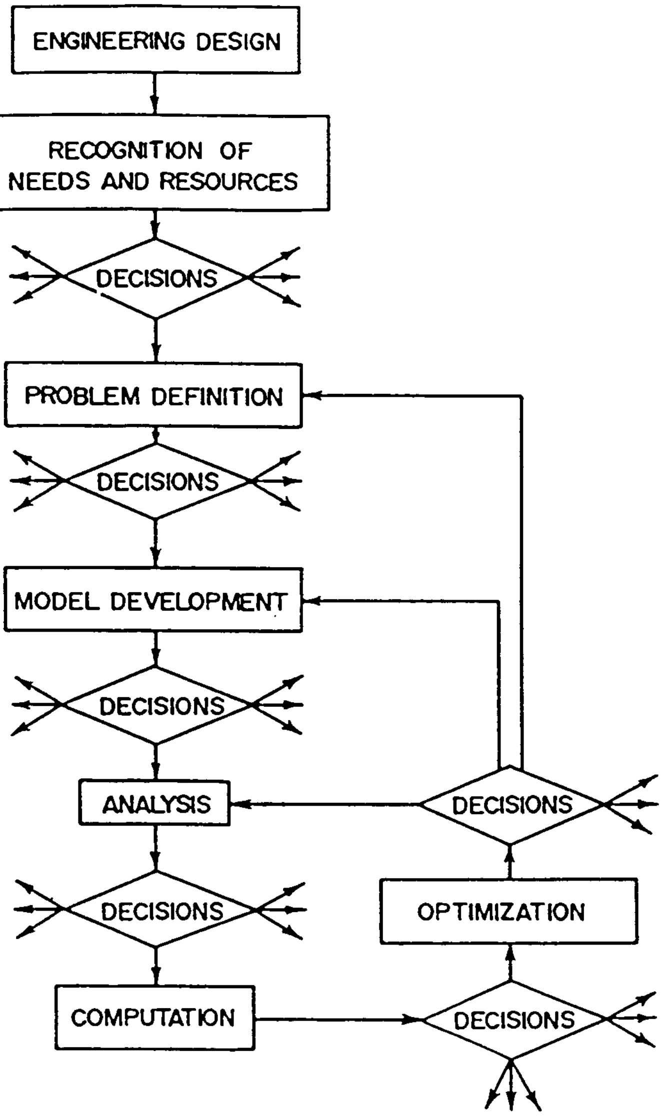

Figure 1. The engineering design process. Source: [1]

$$X = (x_1, x_2, \ldots x_n) \tag{1.1}$$

of design variables to minimize a cost function,

$$f(X) = f(x_1, x_2, \ldots x_n) \tag{1.2}$$

Subject to the equality constraints

$$h_k(X) = h_k(x_1, x_2, \ldots x_n) = 0 \qquad k = 1 \ to \ p \tag{1.3}$$

and the inequality constraints

$$g_j(X) = g_j(x_1, x_2, \ldots x_n) \geq 0 \qquad j = 1 \ to \ m \tag{1.4}$$

where p is the total number of equality constraints and m is the total number of inequality constraints.

The above form of stating the problem is not unique. The optimization problem can be stated in different equivalent statements. One such example is to maximize instead of minimizing the cost function f(X), and also the inequality sign of g(X) can be reversed, so that it is less than or equal to zero. If the problem is to maximize, -f(X) can be minimized and the inequality being positive, the geometric significance at the optimum is equated to the gradients of the objective and all critical constraints point away from the optimum design.

1.4 DESIGN OPTIMIZATION OF GEARS

The design of a gear set is a highly difficult task which involves the satisfaction of many constraints. Savage et al. [5], Carrol et al. [6], and Vanderplaats et al. [7] have published methods for optimum design of spur gear sets. Savage, Coy and Townsend studied the problem of designing a spur gear set of minimum size by considering the interaction of the bending stress and contact stress constraints. Vanderplaats et al., studied the problem of maximizing the mesh life of spur gears. In an interesting paper, Lin and Johnson [8] have proposed a new strategy of incorporating expert systems with optimal spur gear design to overcome the imprecise nature of design parameters. This has opened a new area of research on attaining optimum design by using the techniques of artificial intelligence coupled with numerical algorithms. Tremendous amount of research work is being conducted in the optimal design of other types of gears.

In the Master's thesis of S.N.Muthukrishnan [9], at Portland State University, minimizing the weight of helical gear set using a Random search technique has been discussed. This thesis presents a method to optimize the design parameters of a hypoid gear set.

1.5 OBJECTIVES

Practical hypoid gear design is discussed in many engineering books [10,11]. But it is not a trivial task to apply the available information to produce a good design. The complexity derives from the need to consult various graphs, tables and data. A novice often finds the process difficult to apply. The standard procedure suggested by Gleason Works [11] gives the designer a substantial amount of latitude in choosing some important parameters which are not rigidly defined. Based on this procedure a computer program has been developed to take the burden of the selection and calculation of parameters.

The objective of this project is to develop a software to automate the hypoid gear design process, and using the parameters selected as design variables, optimize the weight of a gear set.

To achieve the objective, the following has to be done.

1. Collect the standard data used in the hypoid gear design process and create data files for them.
2. Interpolate the graphs into polynomial equations for easy implementation with computers.
3. Approximate the geometry of the hypoid gears for volume calculation.
4. Develop the source code for the optimization algorithm, the method of feasible directions.
5. Develop the source code for the simplex linear optimization algorithm, bisection algorithm and golden section algorithm, which are used by the method of feasible directions.

The design objective in this work is taken to be weight optimization; the other objectives that could be considered are, maximizing the mesh life or minimizing the dynamic load.

The design process has been automated; minimizing the art and maximizing the science in order to meet the demands of an increasingly complex world.

1.6 ADVANTAGES AND LIMITATIONS

Application of numerical techniques for mechanical design has advantages and some limitations. The major advantage is the reduction in time spent on design and the systematized logical design procedure which does not depend on intuition and experience. Some of the limitations are, optimization can seldom be guaranteed to give the global design optimum; and most optimization techniques are ill-equipped to deal with discontinuous and highly nonlinear functions. When the number of design variables in the problem increases, the computation time increases and sometimes the cost is prohibitive.

In general, if the techniques are used effectively with the proper understanding of the theory, efficient and economic designs can be achieved. All these optimization techniques can only give an improvement in the design but may not yield the "best" possible. But optimization techniques are valuable tools which, on proper utilization, can improve the existing systems and design methods.

CHAPTER II

THE METHOD OF FEASIBLE DIRECTIONS

2.1 INTRODUCTION

The method of feasible directions is one of the earliest primal methods for solving constrained optimization problems. This method belongs to the group of direction generation methods based on linearization. In this method, rather than relying on an inaccurate linearization to define the precise location of a point, linear approximations are utilized only to determine a locally good direction for search. Along this direction the location of the optimum point could be established by direct examination of values of the original objective and constraint functions, rather than by recourse to the linearized constraints, which lose their accuracy once a departure from the base point is made. This strategy is analogous to that employed in gradient based unconstrained search methods. In that, a linear approximation, i.e. the gradient, is used to determine a direction, but the actual function values are used to guide the search along this direction. In the constrained case, the linearization will involve both objective function and constraints, and the direction generated will have to be chosen to lead to the feasible points.

2.2 BASIC OPTIMUM DESIGN CONCEPTS

The following concepts which are described briefly are discussed in most of the design optimization texts. These are the basic concepts which must be understood properly in order to utilize a numerical optimization technique.

The optimization problem is to find a design in the feasible region which gives a minimum value to a cost function. A function f(x) of n variables has global (absolute) minimum at x^* if

$$f(x^*) \leq f(x) \tag{2.1}$$

for all x in the feasible region. If strict inequality holds for all x other than x^* in the above equation, then x^* is called a strict global minimum. A function f(x) of n variables has a local (relative) minimum at x^* if the above inequality holds for all x in a small neighborhood N of x^* in the feasible region. If strict inequality holds, then x^* is called a strict local minimum. Neighborhood N of the point x^* is mathematically defined as the set of points

$$N = \{ x \mid x \in S \text{ with } \|x - x^*\| < \delta \} \tag{2.2}$$

for some small $\delta > 0$. Geometrically, it is a small feasible region containing the point x^*.

For a graphical explanation of global and local minima, consider graphs of a function f(x) shown in Figure 2. In part(a) of the figure where x is between $-\infty$ and ∞, points B and D are local minima since the function has its smallest value in their neighborhood. Similarly, both A and C are points of local maxima for the function. There is however, no global minimum or maximum for the function since the domain and the function f(x) are unbounded, i.e. x and f(x) are allowed to have any value between $-\infty$ and ∞. If we restrict x to lie between a and b as in part(b) of the Figure 2, then the point E gives the global minimum and F the global maximum for the function.

Weierstrass theorem

The theorem on the existence of global minimum states that if f(x) is continuous on a feasible set S which is closed and bounded, then f(x) has a global minimum in S. A set S is closed if it includes all its boundary points and every sequence of points has a subsequence that converges to a point in the set. A set is bounded if for any point $x \in S$, $x^T x < c$, where c is a finite number. When conditions of the Weierstrass theorem are satisfied, existence of global optimum is guaranteed. But even when the conditions are not satisfied, there still might be a global solution.

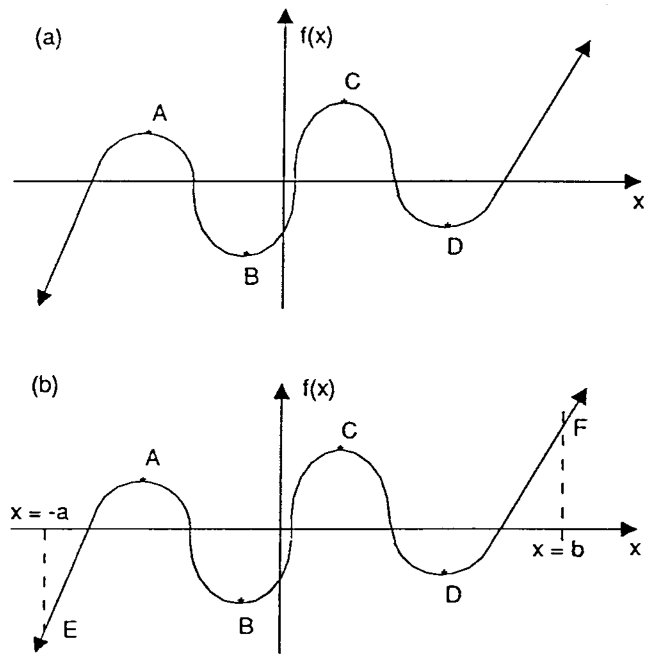

Figure 2. Optimum points. (a) Unbounded domain and function (no global optimum). (b) Bounded domain and function (global minimum and maximum exist). Source: [2]

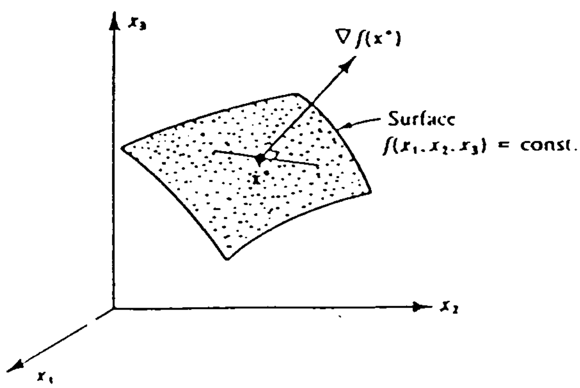

Figure 3. Gradient vector for $f(x_1, x_2, x_3)$ at the point x^*. Source: [2]

Gradient vector

Since the gradient of a function is used in the method of feasible directions to find the feasible search direction, its geometric interpretation is discussed here. Geometrically, the gradient vector is normal to the tangent plane at the point x^* as shown in Figure 3 for a function of three variables. Also, the gradient vector points in the direction of maximum increase in the function. Mathematically, the gradient vector is the partial derivative of a function f(x), where x is any variable. The partial derivative of f(x) is represented as

$$p_i = \frac{\partial f(x)}{\partial x_i} \qquad \text{where} \quad i = 1 \text{ to } n \tag{2.3}$$

The gradient vector is represented as, ∇f, $\partial f/\partial x$, or grad f. Thus, the gradient vector of a function f(x) of n variables at a point x^* is defined as,

$$\nabla f(x^*) = \left[\frac{\partial f(x^*)}{\partial x_1} \; \frac{\partial f(x^*)}{\partial x_2} \; \cdots \; \frac{\partial f(x^*)}{\partial x_n} \right]^T \tag{2.4}$$

where superscript T denotes the transpose of the row vector. Each component of the above gradient vector is a function in itself and must be calculated at the given point x^*.

Status of the constraint at a design point

An inequality constraint can be either active, ε-active, violated or inactive at a given design point. The equality constraint can only be active or violated at the design point. An inequality constraint $g_i(x) \geq 0$ is said to be active at design point x^k, if the constraint value is zero. If the constraint has a positive value then it is called inactive constraint. If it has negative value, then it is called violated constraint. If the constraint value is within a boundary, i.e. $\pm\varepsilon$, where ε is greater than zero, then it is called ε-active constraint.

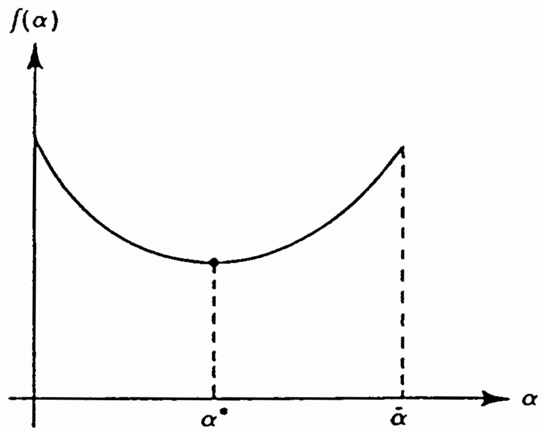

Figure 4. Unimodal function $f(\alpha)$. Source: [2]

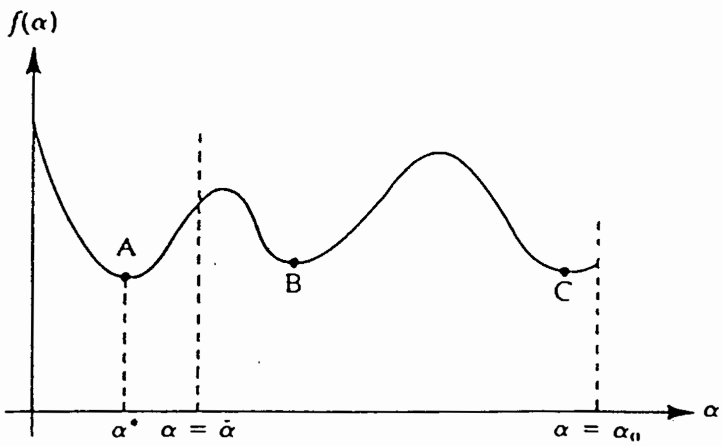

Figure 5. Nonunimodal function $f(\alpha)$ for $0 \leq \alpha \leq \alpha_0$ (unimodal for $0 \leq \alpha \leq \bar{\alpha}$). Source: [2]

Unimodal function

In the method of feasible directions, the multi-variable problem is reduced to a single variable problem in α after finding the direction vector using the basic equation

$$x^{(1)} = x^{(0)} + \alpha d \tag{2.5}$$

where $x^{(0)}$ and d are known. Now the minimum of the univariate function is found which gives the minimum of the multi-variable problem, the values of the updated variables being obtained by substituting the value of α in the above equation. For a univariate function to have a unique minimum within a certain interval, the function must be unimodal. Figure 4 shows the graph of such a function which decreases continuously until the minimum is reached. A function as shown in Figure 5, has many local minima and is thus not a unimodal function. Interval searching methods such as golden section search, are employed easily when the functions are unimodal.

2.3 THE ALGORITHM FOR METHOD OF FEASIBLE DIRECTIONS

The feasible direction method of Zoutendijk [12] has proven to be one of the most efficient algorithms currently available for solving nonlinear programming problems with only inequality type constraints [13]. Since in most mechanical design problems we deal only with inequality type constraints like stress, displacement, etc., this method should be a very good choice for optimization.

First a search vector d is found, and then by moving along this direction, the vector as given in the following equation is updated.

$$x^{i} = x^{i-1} + \alpha^{*} d^{i} \tag{2.7}$$

After determining the search vector, α^{*} is determined using the golden section method.

To reach the minimum, the method follows the constraint boundaries, without necessarily being tangent to them. The method could be easily understood by referring to Figure 6. The gradients of the objective function and constraints are calculated first. Consider the design point

x^0 on the constraint boundary $g_1(x)$. The lines tangent to the line of constant objective and constraint boundary are the linear approximations to the problem. Now a search direction S (or d) has to be found which will reduce the objective function without violating the active constraint for a finite move. Zoutendijk[12] postulated that a direction d would be a good direction for search if it were a descent direction, that is

$$\nabla f(x^{(0)})\ .\ d < 0 \tag{2.8}$$

This direction is feasible if for a small move in that direction, the active constraint is not violated. That is,

$$\nabla g_j(x^{(0)})\ .\ d \geq 0 \tag{2.9}$$

for all constraints $g_j(x)$ that are active at $x^{(0)}$. The direction which satisfies the above inequalities is called a feasible direction. At each iteration, to determine the vector d which will be both a descent and feasible direction, a scalar parameter $\theta > 0$ is introduced such that

$$\begin{aligned} \nabla f(x^{(0)})\, d &\leq -\theta \qquad \textit{and} \\ \nabla g_j(x^{(0)})\, d &\geq \theta \end{aligned} \tag{2.10}$$

and θ is as large as possible. The vector d is normalized by imposing the bounds $-1 \leq d_i \leq 1$, $i = 1,2,\ldots,N$; where N is the number of design variables.

Once finding the direction vector, the next updated value of x could be found by searching on α along the line

$$x = x^{(0)} + \alpha d^{(1)} \tag{2.11}$$

until either the optimum of f(x) is reached or a constraint is encountered. Instead of leaving the α unbounded, a line search on each $g_j(x)$ could be conducted to find the α values greater than zero at which the constraints are bounding. The smallest among the α values called $\bar{\alpha}$ which bind the constraints $g_j(x)$ is chosen. Now, a line search could be conducted to find the α in the range $0 \leq \alpha \leq \bar{\alpha}$ that would minimize $f(x^{(0)} + \alpha d^{(1)})$.

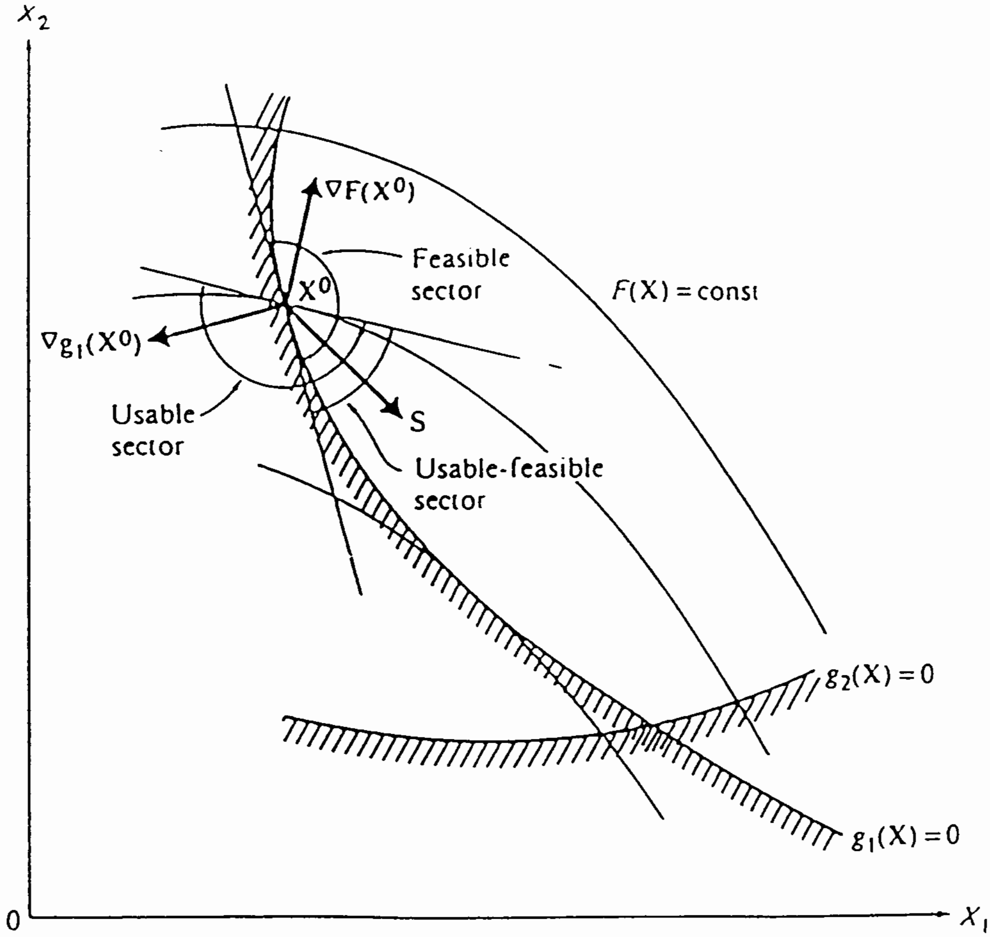

Figure 6. Feasible search direction. Source: [3]

The algorithm is coded in the C language as MOFD.c. The basic algorithm was adopted from [1], and is given below.

Let $I^{(t)}$ be the set of the active constraints at $x^{(t)}$, within some tolerance ϵ, that is,

$$I^{(t)} = \{ j : 0 \leq g_j(x^{(t)}) \leq \epsilon,\ j = 1,2,...,J \} \tag{2.12}$$

for a small $\epsilon > 0$. The following steps give the complete iteration of the feasible direction method.

Step 1: Solve the linear programming problem

Maximize θ

$$\begin{aligned} &\textit{Subject to} \quad \nabla f(x^{(t)})\, d \leq -\theta \\ &\nabla g_j(x^{(t)})\, d \geq \theta \qquad j \,\varepsilon\, I^{(t)} \\ &-1 \leq d_i \leq 1 \qquad i = 1,2,...,N \end{aligned}$$

the solution from above problem is $d^{(t)}$ and $\theta^{(t)}$.

Step 2: If $\theta^{(t)} \leq 0$, then the iteration process terminates, since no further improvement is possible. Otherwise, determine

$$\bar{\alpha} = \min\{ \alpha : g_j(x^{(t)} + \alpha d^{(t)}) = 0,\ j = 1,2,...,J \text{ and } \alpha \geq 0 \}$$

if no $\bar{\alpha} > 0$ exists, set $\bar{\alpha} = \infty$.

Step 3: Find $\alpha^{(t)}$ by line search, such that

$$f(x^{(t)} + \alpha^{(t)} d^{(t)}) = \min\{ f(x^{(t)} + \alpha d^{(t)}) : 0 \leq \alpha \leq \bar{\alpha} \}$$

Using the $\alpha^{(t)}$ value, set $x^{(t+1)} = x^{(t)} + \alpha^{(t)} d^{(t)}$ and continue the iteration.

In the computer code of the algorithm, the search direction was found using the simplex method of optimization. The search for the boundary and the line search for the optimum are found using the bisection and golden-section search methods respectively. The partial derivatives of the gradient vector are found using the central difference method. The method can be simply stated as,

$$f'(x) = \frac{f(x + \Delta s) - f(x - \Delta s)}{2\Delta s} \quad (2.13)$$

where f'(x) is the numerical derivative at the value of x and Δs the small increment.

2.4 FINDING SEARCH DIRECTION BY SIMPLEX METHOD

The direction finding problem in the step 1 of the feasible direction method algorithm is solved using the modified simplex method. The basic algorithm and the computer code in C language of this method, are adopted from Numerical Recipes [14]. The only restriction in applying the method to the direction finding problem is the normalizing constraint on d,

$$-1 \leq d_i \leq 1 \qquad i = 1,2,...,N$$

where N is the number of design variables. Since the simplex method's standard form needs the value of d_i to be greater than zero, the above constraints can be changed to the following form,

$$\text{Let,} \quad d_i = d_i^{new} - 1$$

$$d_i^{new} \leq 2$$

The new value of d_i is substituted in the problem and solved for the variables d_i^{new} and θ. After finding the d_i^{new} values they are again substituted in the above equation to get the real values of the direction vector.

The feasible vector that maximizes the objective function is called the optimal feasible vector. This vector can fail to exist for two reasons,

1. there are no feasible vectors, i.e. the given constraints are incompatible. In this case the constraints could be rewritten in a different format and tested again for solution.
2. there is no maximum, i.e. the maximum of the objective function can go to infinity, giving an unbounded solution while still the constraints are satisfied. In this case the problem is under-constrained and could be overcome by putting additional constraints on the variables.

2.5 THE BISECTION ALGORITHM

The bisection method is used in finding the boundary of the feasible region. The appropriate α values when the constraints become bounding, i.e. $g_i(x) = 0$ is found and used for finding the minimum in the line search. The bisection method is based on the intermediate value theorem. For a continuous function, defined on the interval [a,b] such that f(a) and f(b) of opposite sign, then there exists p, $a < p < b$, for which $f(p) = 0$. The method works by repeated halving of subintervals of [a,b] and, at each step, locating the "half" containing p. The basic algorithm is given below.

```
Step 1:     Set i = 1
Step 2:     while i ≤ N
            Step 3  Set p = a + (b - a)/2
            Step 4  If f(p) = 0 or (b - a)/2 < TOL then
                              Output p;
                              End
            Step 5  Set i = i + 1
            Step 6  If f(a).f(p) > 0 then a = p
                    Else b = p
                    Goto step 2
Step 7      Output ("The method failed for N iterations, N =",N);
            Output ("Repeat the procedure by changing the N value");
            Stop.
```

The inputs are the bounds a,b, the tolerance TOL and the maximum number of iterations N. The above inputs can be changed appropriately to get the correct solution. This algorithm is coded as Bisect.c. After finding the α values for the different binding constraints, the smallest α is selected and is called $\bar{\alpha}$.

2.6 THE GOLDEN SECTION SEARCH METHOD

The third step in the basic algorithm of the method of feasible directions is the line search to find the minimum. The golden section method is chosen for the line search to find the minimum because of its proven advantages. This method is easily programmed on digital computers. The function is assumed to be unimodal and need not have continuous derivatives. The rate of convergence of this method is known, as compared to polynomial or curve-fitting techniques.

The lower and upper bounds of the variable α are 0 and $\bar{\alpha}$ and these bounds will be called as X_l and X_u respectively. The corresponding function values at these bounds are also to be evaluated. Now two intermediate points X_1 and X_2 are picked, such that $X_1 < X_2$ and functions are evaluated at these points to provide F_1 and F_2. Since the function is unimodal, the values of either X_1 or X_2 will form a new bound on the minimum.

The values of X_1 and X_2 are defined as follows.

$$
\begin{aligned}
X_1 &= (1-\tau)X_l + \tau X_u \\
X_2 &= \tau X_l + (1-\tau)X_u
\end{aligned}
\tag{2.14}
$$

The ratio X_2 to X_1, called the golden section number, is given as

$$
\frac{X_2}{X_1} = 1.61803 \tag{2.15}
$$

and the value of $\tau = 0.38197$.

The golden section search is coded as Golden_search.c. This is written as a function and called by the main program MOFD.c. The flowchart of the algorithm is given in Figure 7.

For all numerical methods a criterion must be defined to know when the process has converged. The initial interval of uncertainty, X_u-X_l is reduced to some fraction ϵ of initial interval or some specific magnitude Δx. The ϵ is referred to as a relative tolerance, dependent on the initial interval and Δx as the absolute tolerance which is independent, the value being selected as 0.0001.

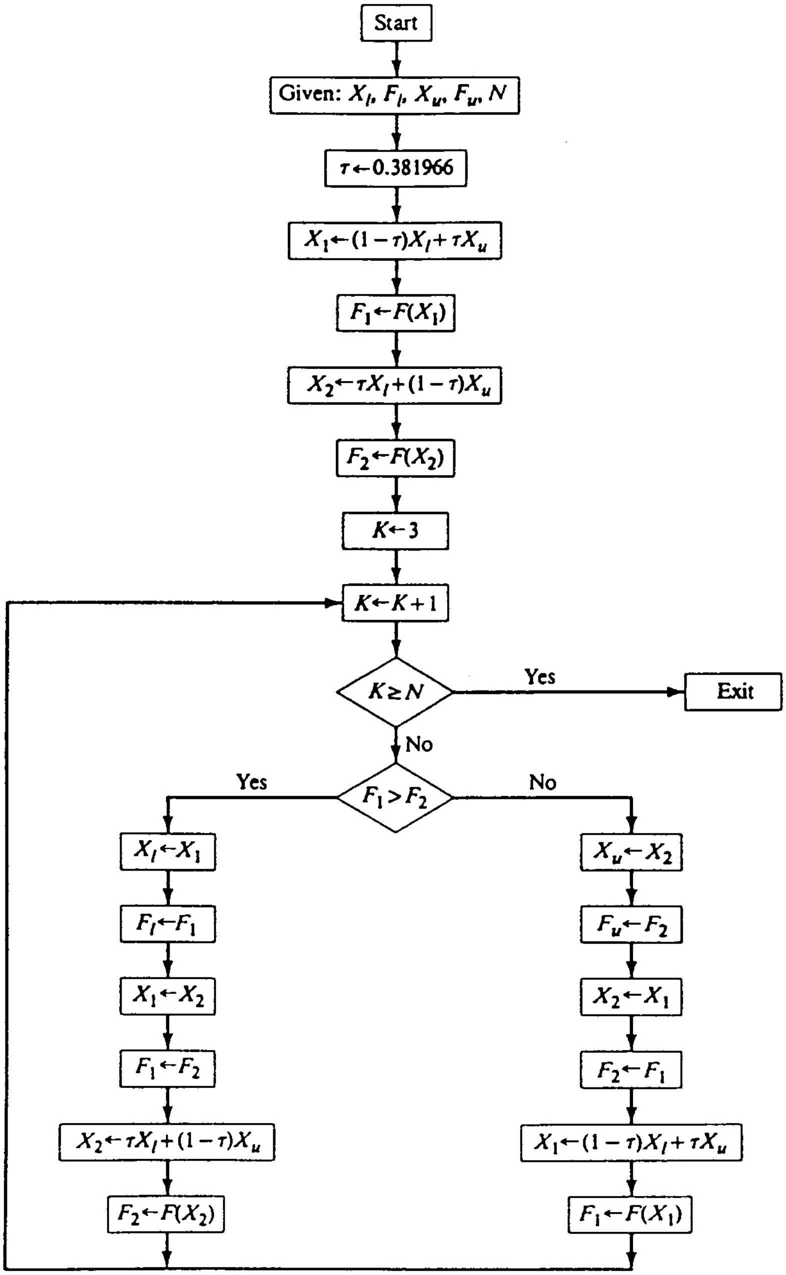

Figure 7. Golden section search algorithm. Source: [3]

The relative tolerance is calculated from the absolute tolerance as,

$$\epsilon = \frac{\Delta x}{X_u - X_l} \tag{2.16}$$

This relative tolerance ϵ is converted to a maximum number of function evaluations in addition to the three required to evaluate F_l, F_1, and F_u. The interval is reduced by the fraction τ(0.38197) on every iteration. Thus the tolerance can be expressed as

$$\epsilon = (1 - \tau)^{N-3} \tag{2.17}$$

where N is the total number of function evaluations. Solving the above equation we get

$$N = \frac{\ln \epsilon}{\ln (1 - \tau)} + 3 = -2.078 \ln \epsilon + 3 \tag{2.18}$$

The value of N is used as a convergence criterion in terminating the iteration process.

2.7 TOPKIS - VEINOTT VARIANT

In the basic algorithm of the feasible direction method, the successive direction-generating subproblems differ in the active constraint set $I^{(l)}$ used at each iteration. This aids in reducing the size of the linear programming problem. Since, the only constraints considered are the ones binding at the current feasible point, a zig-zag pattern results, which slows down the progress towards the minimum and converges to points that are not Kuhn-Tucker points. This is known as jamming, and occurs when the steps taken become shorter and shorter as direction vector d alternates between closely adjacent boundaries. The steps become shorter not because optimum is reached but due to a nearby constraint not considered when the direction finding sub-problem is encountered.

To overcome the problem, an alternative approach Topkis-Veinott variant method [15] is used. In this method the active constraint concept is replaced with the direction-finding subproblem as follows:

Maximize θ

Subject to $\nabla f(x^{(t)})d \leq -\theta$

$$g_j(x^{(t)}) + \nabla g_j(x^{(t)})d \geq \theta \qquad j = 1,2,\ldots,J$$

$$1 \geq d \geq -1$$

The remaining algorithm is unchanged. The primary difference in the subproblem definition is the inclusion of the constraint value in the inequality associated with each constraint. If the constraint is loose at $x^{(t)}$, i.e. $g_j(x^{(t)}) > 0$, then the selection of d is less affected by this constraint, because the positive constraint value will counterbalance the effect of the gradient term. This method, as proved by Topkis [15], ensures that no sudden changes are introduced in search direction as constraints are approached, thus jamming is avoided. In the computer code of the algorithm MOFD.c this approach is incorporated thus ensuring that the minimum is reached faster.

2.8 EXAMPLE PROBLEM

The following problem from [1] is solved using the computer code of the feasible direction method MOFD.c and the results were found to be very close to the theoretical results. The problem and results are given below.

$$\textit{Minimize} \quad f(x) = (x_1 - 3)^2 + (x_2 - 3)^2$$

$$\textit{Subject to} \quad g_1(x) = 2x_1 - x_2^2 - 1 \geq 0$$

$$g_2(x) = 9 - 0.8x_1^2 - 2x_2 \geq 0$$

Initial values of $x_1 = 1$, $x_2 = 1$, $f(x) = 8.0$

TABLE I

ITERATION HISTORY

Iteration No.	x_1	x_2	f(x)
0	1.0	1.0	8.0
1	2.179487	0.606838	6.400467
2	2.477958	1.988929	1.294793
3	2.503471	1.993010	1.260569
4	2.4985	1.99924	1.253032

TABLE II

COMPARISON OF RESULTS

	x_1	x_2	Minimized f(x)
Theoretical	2.50	2.0	1.250
Method of Feasible Directions	2.4985	1.99924	1.253032
% Difference	0.06	0.04	0.242

CHAPTER III

HYPOID GEAR DESIGN

3.1 INTRODUCTION

Hypoid gears are similar to spiral bevel gears except that the pinion axis is offset above or below the gear axis. If there is sufficient offset, the shafts can pass one another and a compact straddle mounting can be used. Unlike spiral bevels, the hypoids should have non-symmetrical profile curvatures for proper tooth action, so the pressure angles on the two sides are unequal. Hypoid pinion has a larger spiral angle than the gear. Since the normal pitch in both members should be the same for mating, the transverse pitch in the hypoid pinion is greater. This makes the hypoid pinion larger in size, therefore stronger than the corresponding spiral bevel pinion. Moreover, the hypoids have a lengthwise sliding action, the amount being a function of the difference between the spiral angles on the pinion and gear.

Hypoid gears, like bevel gears, can be used for transmitting power between shafts at practically any angle and speed. But they are especially recommended when the peripheral speeds are in excess of 1000 feet per minute or 1000 rpm, whichever occurs first. They can be used at lower speeds, if extreme smoothness and quietness are required. When used for large reduction ratios, hypoid gears can achieve a substantial reduction in size. The main advantages of hypoid gears over spiral bevel gears are that the pinion can be made stronger for the same ratio, and the shafts do not intersect.

Hypoids are almost universally used in automobiles, and to some extent in trucks, because of their smoother operation and greater size and strength, which allows higher reduction ratios while still maintaining the required pinion shank size. Together with the shank offset, the hypoid set assists in lowering the car body, which is an additional advantage. In precision machine tool applications, hypoids are used instead of worm gears when the ratio exceeds 10 to 1, because of their better accuracy.

3.2 DESIGN CONSIDERATIONS

Hypoid gears are suitable for transmitting power at practically any angle and speed. The power, speed, gear ratio and operating conditions must be defined as the first step in designing a gear set for the specific application. The operating condition requirements are the following.

1. Application - whether the gear to be used in automotive or non-automotive field.
2. Mounting conditions - i) Both members straddle mounted
   ii) One member straddle mounted
   iii) Neither member straddle mounted (both overhung).
3. Whether the gear is to be ground for finishing.
4. Type of loading on the prime-mover and the driven member : uniform, medium shock, or heavy shock.
5. Type of material to be used [Appendix A].

From the above inputs, gear pitch diameter is estimated based on the gear torque using the graph in Appendix B. The charts are based on case-hardened steel and if the material and heat-treatment is different, then the estimated gear size must be multiplied by the material factor given in Appendix A. If the gear is to be ground, then the size is multiplied by 0.80. Pinion pitch diameter is obtained, by dividing the gear diameter by the speed ratio. Using the pinion pitch diameter, number of teeth and facewidth can be estimated using tables and graphs in Appendix A and B. The diametral pitch is now calculated as the ratio of number of gear teeth to gear pitch diameter. Hypoid offset in general should not exceed 25 percent of the gear pitch diameter for power drives and for very heavily loaded gears must be limited to 12.5 percent of gear pitch diameter. As a good approximation, suggested by Gleason Works [11], the maximum allowable values are considered for offset. The pressure angle is unbalanced on both sides of a gear tooth in order to produce equal contact ratios on two sides. For automotive and light duty drives, 19° is used, and for heavy duty drives, 22.5° is used, as average pressure angles.

3.3 CONTACT AND BENDING STRENGTH

The rating formulas given below are specifically prepared for hypoid gears in which the tooth contact pattern has been developed to give good results in the final mounting under full load. The design procedure was developed by Gleason Works [11] and is widely accepted in the industry circles.

The basic equation for contact stress in a hypoid gear or pinion is,

$$S_c = C_p \sqrt{\frac{2T_{pmax} C_o}{C_v F D^2} \frac{N^2}{n^2} \frac{C_s C_m C_f}{I}} \sqrt[3]{\frac{T_p}{T_{pmax}}} \tag{3.1}$$

The basic equation for bending stress in hypoid gear is

$$S_t = \frac{2T_G K_o}{K_v} \frac{P_d}{F_G D} \frac{K_s K_m}{J_G} \tag{3.2}$$

for diametral pitches less than 16, $K_s = \dfrac{1}{P_d^{\,0.25}}$

for diametral pitches greater than 16, $K_s = 0.5$

where,

S_c = calculated contact stress at point on tooth where its value will be maximum, lb/in²

S_t = calculated tensile bending stress at root of gear teeth, lb/in²

C_p = elastic coefficient of the gear and pinion materials combination, √lb/in

T_P, T_G = transmitted torques of pinion and gear, respectively, lb-in

T_{pmax} = maximum transmitted pinion torque lb-in

K_o, C_o = overload factors for strength and durability, respectively

K_v, C_v = dynamic factors for strength and durability, respectively

K_s, C_s = size factors for strength and durability, respectively

K_m, C_m = load distribution factors for strength and durability, respectively

C_f = surface condition factor for durability

I = geometry factor for durability

J = geometry factor for strength.

The elastic coefficient for hypoid gears with localized tooth contact pattern is given by

$$C_p = \sqrt{\frac{3}{2\pi} \frac{1}{\frac{1-\mu_p^2}{E_p} + \frac{1-\mu_G^2}{E_G}}} \tag{3.2}$$

where, μ_p, μ_G = Poisson's ratio for materials of pinion and gear, respectively. Since all the materials considered are ferrous, a value of 0.30 is used.

E_p, E_G = Young's modulus of elasticity for materials of pinion and gear, respectively. For steel, 30.0×10^6 lb/in^2 is used.

The transmitted torque in pound inches is calculated directly from the power transmitted and is given as follows.

$$Torque = \frac{63000\,P}{N}$$

where, P = power transmitted in hp

N = speed in rpm of gear or pinion.

The maximum transmitted pinion torque is calculated using the above equation by selecting the corresponding values of power, and pinion speed.

The overload factors K_o and C_o, makes allowance for the roughness or smoothness of operation of both the driving and driven units. In determining the overload factor, consideration should be given to the fact that many prime-movers develop momentary overload torques which are very much greater than the rated normal operating torque. The overload factor table in Appendix A is used for selecting the factor.

The dynamic factors K_v & C_v, reflect the effect of inaccuracies in profile, tooth spacing, and runout on instantaneous tooth loading. If the accuracy of the hypoid gear is AGMA Class 11 or higher, then the dynamic factor can be taken as unity from curve no. 1 of dynamic factor graph in Appendix B. Otherwise for lower accuracy gears the dynamic factor can be obtained from Curve no. 2.

The size factors K_s & C_s, take into account the fact that the allowable stress is a function of the size of the specimen and the hardenability of the material. The effect of specimen size shows up most clearly on the allowable bending stress; and less noticeable on the allowable contact stress. The size factor for durability is taken as 1.0.

Performance of the hypoid gears is dependent to a considerable degree upon their alignment under operating conditions, the load distribution factors K_m & C_m, is introduced in the rating formulas to make allowance for this effect. This factor is based on the magnitude of the relative displacements of the gear and pinion and is selected from the load distribution factor table in Appendix A.

The surface condition factor for durability C_f , depends on surface finish as affected by cutting, lapping, grinding, shot peening, etc. On the assumption that first class gear manufacturing practice is followed, the surface condition factor is taken as unity.

The geometry factor for durability I, incorporates the relative radius of curvature between mating tooth surfaces, the load location, the load sharing between pairs of teeth, the effective facewidth, and the inertia factor resulting from a low contact ratio. The series of graphs in Appendix B gives the durability geometry factors for some of the most commonly used gear sets.

The geometry factor for strength J, incorporates tooth form factor, the load location, the load sharing between pairs of teeth, the effective facewidth, the stress concentration and stress correction factors, and the inertia factor resulting from a low contact ratio. The series of graphs in Appendix B gives the strength geometry factors for some of the most commonly used gear sets.

The graphs of geometry factor I and J are converted to polynomial equations of the following form to get the appropriate values. The intermediate values can be obtained by interpolation or extrapolation.

$$I \text{ or } J = a_0 + a_1 n + a_2 n^2 + a_3 n^3 + \ldots + a_n n^n$$

The converted polynomial equations are plotted against the number of pinion teeth, to verify their accuracy with the original curves. For a correlation of 90% to 99% the order of polynomials obtained for the geometry factors ranged from 5 to 10. The order of the polynomial equations were increased if their accuracy is not atleast 90%.

CHAPTER IV

OPTIMIZATION PROBLEM AND RESULTS

4.1 HYPOID GEAR DESIGN AS OPTIMIZATION PROBLEM

The traditional hypoid gear design procedure is similar to the design cycle of a mechanical component. In general, mechanical design begins with an estimate of the size of the component based on power transmitted, load capacity or physical conditions, etc. After making a good estimate, the component's specifications are analyzed to satisfy various constraints it has to undergo in practical situation. If the estimate does not satisfy the constraints, then the value has to be properly adjusted and the analysis must be done again to check the constraints. This procedure is repeated until we get a satisfactory design.

By using an optimization technique, the preliminary estimation and detailed design mentioned above are replaced with a numerical search algorithm. The major advantage of using an optimization method is that once specifications and constraints are given, the numerical search algorithm can utilize this information and automatically search through the design space defined by the geometric variables (design variables).

The common design objective for hypoid gears is weight minimization. The hypoid gear design problem can be stated in a general design optimization form as follows.

Minimize,

Weight = Density x Volume

Subjected to

1. Contact stress constraint

2. Bending stress constraint

3. Facewidth constraint

and the side constraints on the design variables based on manufacturing process are,

1. Facewidth, $F \geq 1.0$ inches
2. Number of gear teeth, $N \geq 5$
3. Diametral pitch, $P_d \geq 1.0$

Contact Stress Constraint

The calculated contact stress due to the loading must be equal to or less than the allowable contact stress of the material to avoid surface failure, i.e.

$$S_c \leq S_{ac}$$

The equation 3.1 gives the value for calculated Sc. The allowable contact stress for different gear materials is given in the Table XII in Appendix A.

Bending Stress Constraint

The calculated bending stress due to the loading must be equal to or less than the allowable bending stress of the material to avoid failure in bending, i.e.

$$S_t \leq S_{at}$$

The equation 3.2 gives the value for calculated S_t. The allowable bending stress for different materials is given in the Table XIII in Appendix A.

Facewidth Constraint

The facewidth of the hypoid gear should be limited to

$$F \leq \frac{10}{P_d}$$

Increasing the facewidth adds the strength and durability theoretically, but at a rapidly diminishing rate. This causes manufacturing difficulties by requiring cutters of less point width and decreases possible fillet radii. It can also increase the possibility of breakage and wear if the load becomes concentrated on the smaller end of the teeth.

Volume of the gear

The volume of the hypoid gear is approximated by a geometry having two truncated cones with a common base diameter. The half angle of the cone is the pitch angle and mean pitch diameter is considered as the base diameter. Since hypoid gear geometry is quite complicated and very difficult to deal with analytically, some assumptions have to be made in the approximations, and are mentioned below. As can be seen from the parameters in the volume equation, reduction in the facewidth will lead to the reduction of volume.

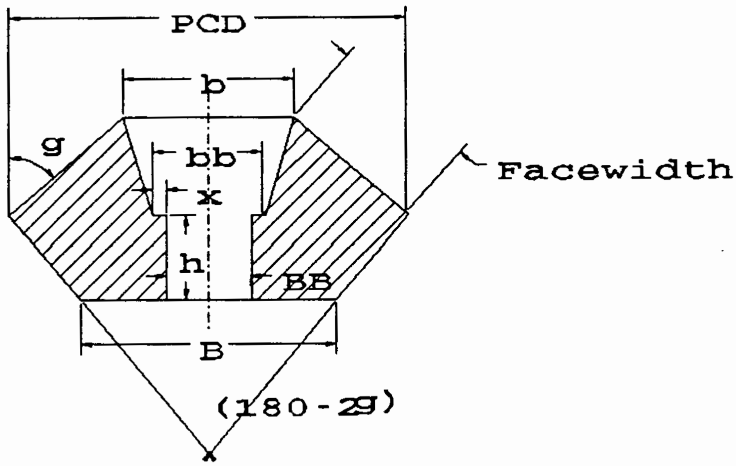

Figure 8. Hypoid gear geometry for volume calculation.

Let,

g = gear pitch angle

x = 0.1 x Pitch circle diameter

h = F cos(g)

The total volume can be calculated by considering the gear as two truncated cones having common base diameter and placed as shown in the Figure 8. The volume of the top truncated cone can be calculated by subtracting the volumes of the full cone and the truncated cone having base diameter as b, from the full cone having base diameter of PCD.

The parameters shown in the figure can be calculated as follows.

$$B = PCD - 2\left(\frac{h}{\tan(g)}\right)$$

$$b = PCD - 2F\sin(g)$$

$$bb = b - 2\frac{F\cos(g)}{\tan(g)}$$

$$BB = bb - 2x$$

Top full cone volume, having base diameter PCD

$$X1 = \frac{1}{3}\pi\left(\frac{PCD}{2}\right)^2\frac{PCD}{2\tan(g)}$$

Top full cone volume, with base diameter b

$$X2 = \frac{1}{3}\pi\left(\frac{b}{2}\right)^2\frac{b}{2\tan(g)}$$

Truncated cone volume, with base diameter b

$$X3 = \left[\frac{1}{3}\pi\left(\frac{b}{2}\right)^2\frac{b\tan(g)}{2}\right] - \left[\frac{1}{3}\pi\left(\frac{bb}{2}\right)^2\frac{bb\tan(g)}{2}\right]$$

Bottom full cone volume, with base diameter PCD

$$X4 = \frac{1}{3}\pi\left(\frac{PCD}{2}\right)^2\frac{PCD\ \tan(g)}{2}$$

Bottom cone volume, with base diameter B

$$X5 = \frac{1}{3}\pi\left(\frac{B}{2}\right)^2\frac{B\tan(g)}{2}$$

Cylinder volume, with diameter BB and height h

$$X6 = \pi \left(\frac{BB}{2}\right)^2 h$$

Now the total volume can be calculated from the above quantities.

Total gear volume = X1 - X2 - X3 + X4 - X5 - X6

Volume of the pinion

The Hypoid pinion geometry is much simpler compared to the gear for calculating the volume. The volume of the pinion is calculated as a truncated cone having base diameter of pinion PCD.

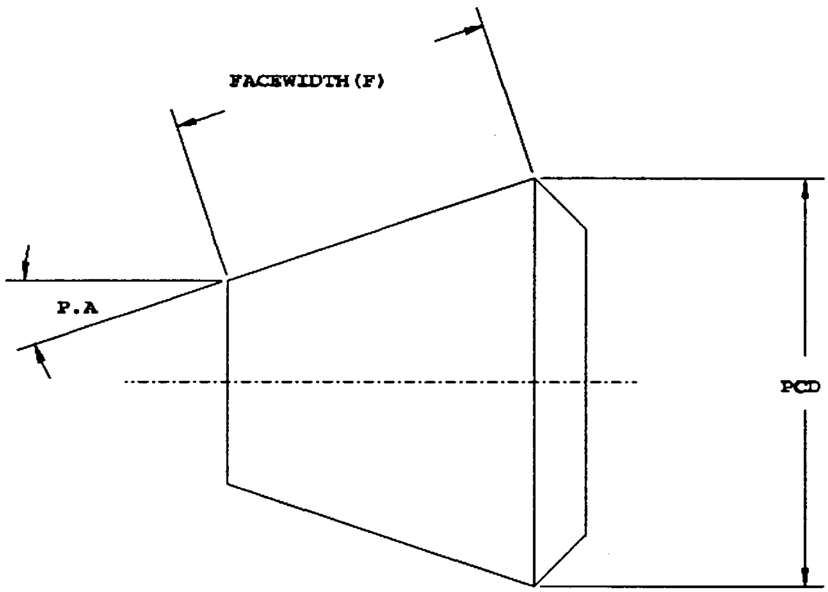

Figure 9. Hypoid pinion geometry for volume calculation.

Let,

P.A = Pinion pitch angle

$$Volume = \frac{1}{3}\pi \left(\frac{PCD}{2}\right) \frac{PCD}{2\tan(P.A)} - \frac{1}{3}\pi \left[\frac{PCD - 2F\sin(P.A)}{2}\right]^2 \left[\frac{PCD}{2\tan(P.A)} - F\cos(P.A)\right]$$

The pinion and gear pitch angles are calculated using the formulas given in Table XIV. The pinion facewidth and pitch circle diameter are also calculated using the formulas in Table XIV.

4.2 DESIGN PROBLEM AND RESULTS

The Hypoid gear CAD procedure has been extensively tested for a large number of industrial and automotive designs. The efficiency of the Feasible Directions method, directly depends on the starting solution lying within the feasible domain. Since most of the parameters are chosen from standard tables, the starting solutions are nearer to the optimal point, thus enhancing the computational efficiency. A typical design example is presented here.

Problem

Transmitted power : 350 HP

Input pinion speed : 2100 RPM

Gear ratio : 4

Other requirements

1) The gear is to be used for industrial application.
2) One member is straddle mounted.
3) The gear should be ground for finishing.
4) Loading on the prime-mover and the driven member is with heavy shock.
5) Material to be used is oil hardened steel of 400 BHN for both gear and pinion.

Results

Using the input data, allowable bending and contact stress values are read from the data files. Initial values of design variables are selected and appropriate correction factors are applied to them. The results of the optimization is presented in Table III and IV.

TABLE III

OPTIMIZATION RESULTS

Iteration	Gear teeth (N)	Diametral pitch (Pd)	Facewidth (F), in.	Gear weight (lb)
Initial	56	3.355	2.560	43.580
1	56	3.635	2.751	42.779
2	56	3.723	2.739	40.970
3	56	3.692	2.709	40.836
4	56	2.141	1.164	28.253
5	56	2.141	1.164	28.253

The results show the weight of the gear has been reduced by 35.17%. The overall weight reduction of the gear-pinion set is 18.7%, which is significant. The design variables, diametral pitch(Pd) and gear facewidth(F) have reduced considerably while the number of gear teeth did not experience any change. Since the gear teeth values are selected from a table which gives the field tested values, the optimization program could not reduce it further. The table values can be accepted as optimum, since their inclusion as design variable did not change the optimization path. Also this shows that to reduce the weight it is enough to consider facewidth and diametral pitch as the design variables. But this may not be the case for all applications.

Figure 10, shows the contour plots of the constraints with facewidth and diametral pitch as the variables. This plot is drawn for the above example and only the feasible region is shown. The plots show that the contact stress constraint does not play any role on the minimization. The entire optimization process is constrained only by the bending stress constraint and the width constraint. Figures 11, 12 and 13, show the change in design variables and the weight.

A comparison between the initial selected values and the final optimized values is given in Table IV.

TABLE IV

COMPARISON BETWEEN INITIAL AND OPTIMIZED VALUES

Parameter	Initial value	Optimized value
Number of gear teeth	56	56
Number of pinion teeth	14	14
Diametral pitch	3.355	2.141
Gear facewidth (in.)	2.560	1.164
Pinion facewidth (in.)	3.870	1.580
Gear pitch diameter (in.)	16.690	25.040
Pinion pitch diameter (in.)	4.380	7.150
Weight of gear (lb)	43.580	28.253
Weight of pinion (lb)	9.000	14.520
Bending stress (lb/in^2)	44887.820	49999.910
Contact stress (lb/in^2)	128632.060	135100.690
Allowable bending stress (lb/in^2)	50000.000	
Allowable Contact stress (lb/in^2)	180000.000	

4.3 CHECK FOR KUHN-TUCKER OPTIMALITY CONDITIONS

Kuhn-Tucker conditions are the necessary and sufficient conditions for checking the optimality criteria for both nonlinear equality and inequality constrained problems. The Kuhn-Tucker problem formulation given in [1] is used to check the optimal solution obtained in hypoid gear design problem. For the optimum design vector x^*,

$$\nabla f(x^*) - \sum_{j=1}^{3} u_j \nabla g_j(x^*) = 0$$

$$g_j(x^*) \geq 0$$

$$u_j g_j(x^*) = 0$$

$$u_j \geq 0$$

$$for, \quad j = 1,2,3$$

At optimum the contact stress and facewidth constraints are inactive. Only bending stress constraint is active. The Lagrange multiplier for the inactive constraints is zero to satisfy Kuhn-Tucker conditions. Now, the Kuhn-Tucker condition at optimum becomes,

$$\nabla f(x^*) - u_{bending} \nabla g_{bending}(x^*) = 0$$

Substituting the gradient values at x^*,

$$(0.83 - 21.71 + 32.88) = u_{bending} (1080.74 - 37528.26 - 42949.54)$$

$$u_{bending} = 1.845 \times 10^{-3} > 0$$

$$\text{and,} \quad u_{bending} g_{bending}(x^*) = 0$$

The above equations prove that Kuhn-Tucker optimality conditions are satisfied at optimum for the hypoid gear problem.

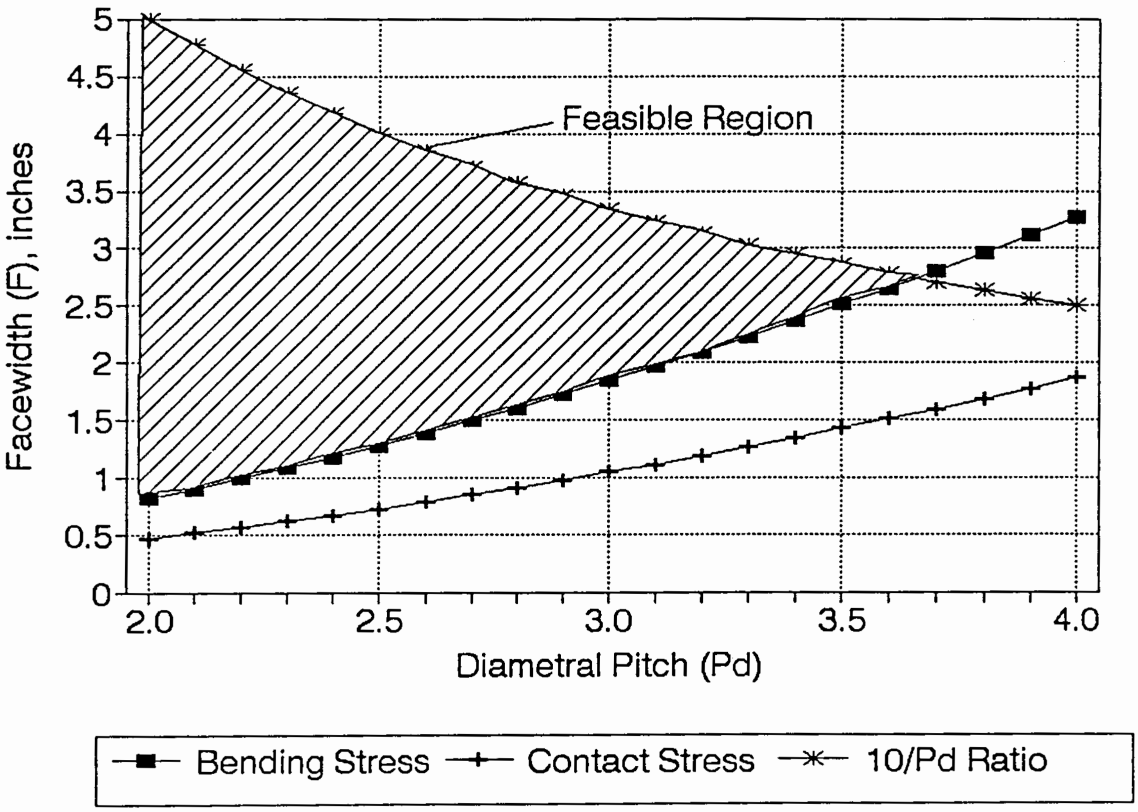

Figure 10. Contour plot.

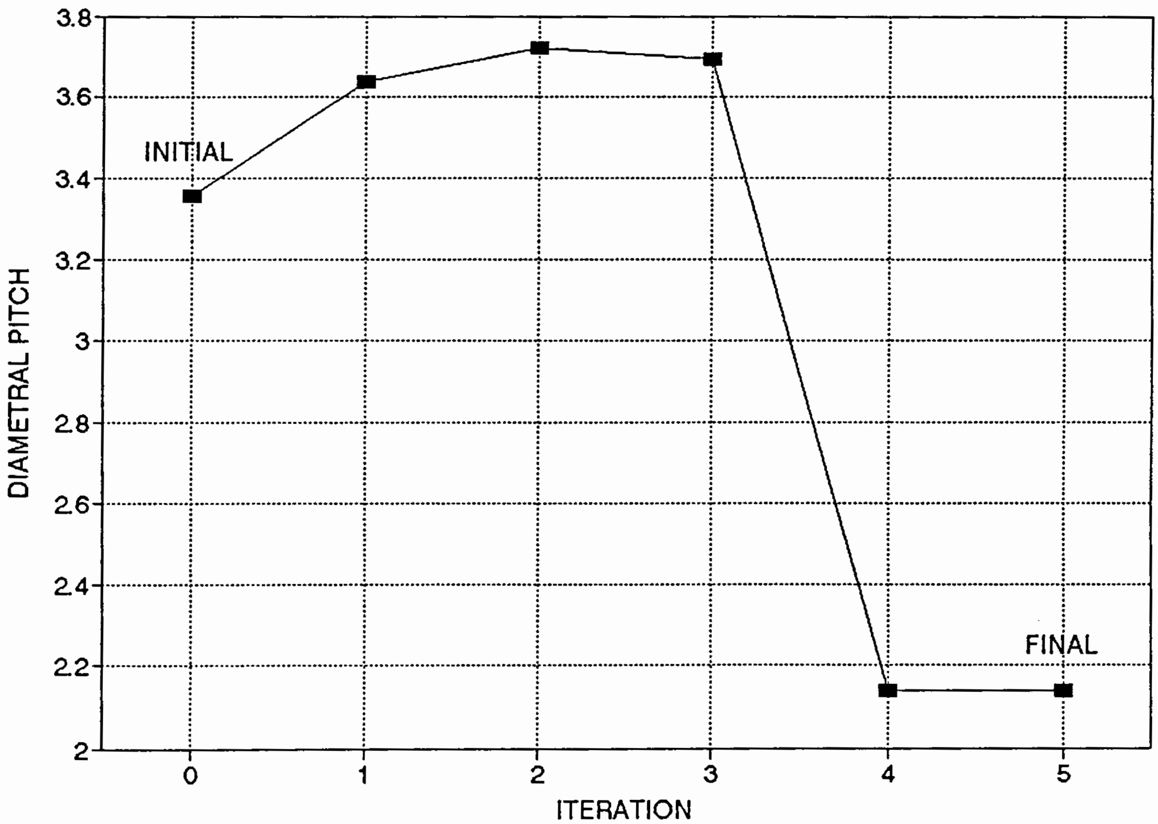

Figure 11. Iteration vs. Diametral pitch.

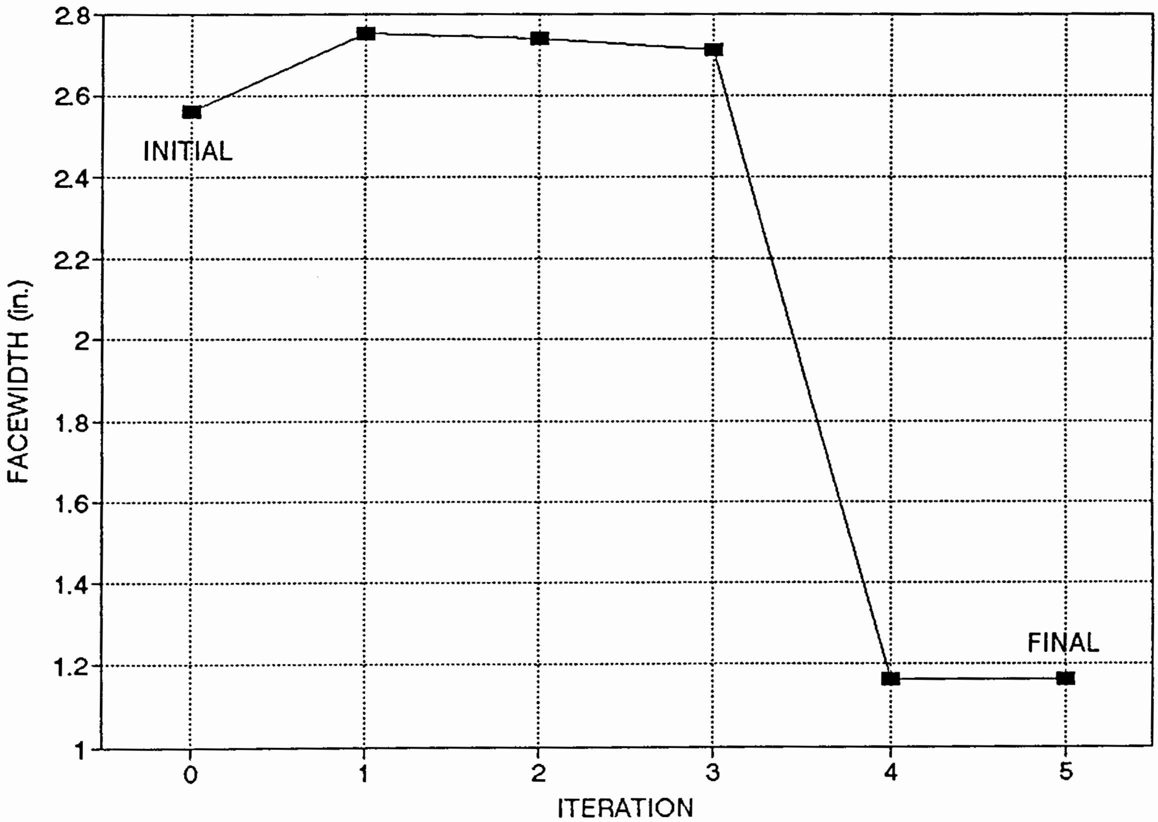

Figure 12. Iteration vs. Facewidth.

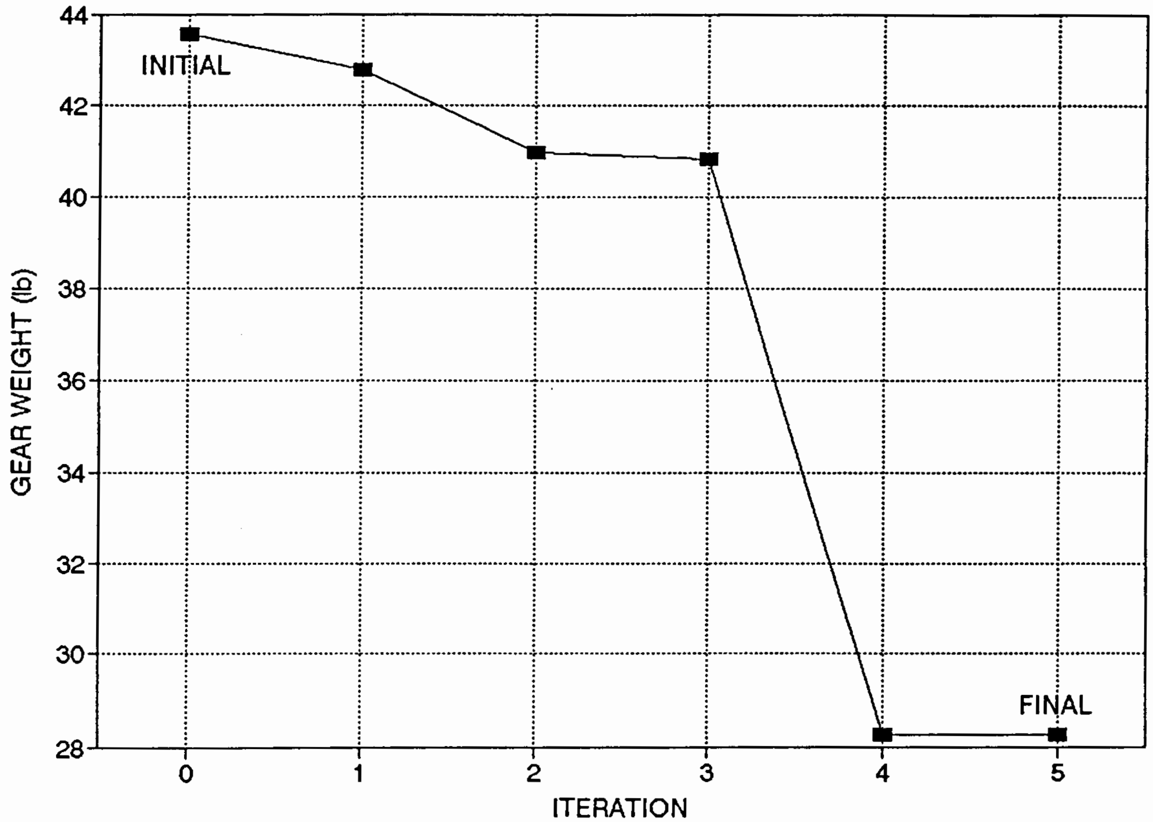

Figure 13. Iteration vs. Gear weight.

CHAPTER V

CONCLUSION

The methodology applicable to constrained optimization problem has been studied and tested with examples. Considerable amount of time is devoted to the discussion of formulation of problem and to the computational devices expediting the solutions. The design of hypoid gears has been addressed as a numerical optimization task. The objective here was to demonstrate the use of optimization techniques for a design problem and to show the improved results. The development of software consistent with the theoretical concepts was necessary to achieve this goal. A test problem was given to demonstrate the applicability to typical hypoid gear design problem.

The use of numerical optimization has been shown, for the improved design of gears with less weight as the main criterion. In some cases, special algorithms must be used to obtain feasible starting points if they are not known. This could be done as a future extension of this work to make the algorithm more effective for applications where starting points are not feasible.

The example provided here is considered sufficient to indicate the breadth of application of optimization techniques for mechanical component design. This also presents the importance and understanding of problem definition and analyzing the final results. It is hoped that this work provides stimulation toward the expanded application of these techniques in practical engineering design problems.

REFERENCES

[1] Reklaitis, G.V., Ravindran, A., and Ragsdell, K.M.," Engineering Optimization: Methods and Applications", John Wiley & Sons, 1983.

[2] Arora, Jasbir S.,"Introduction to Optimum Design", McGraw-Hill, 1989.

[3] Vanderplaats, Garret N.,"Numerical Optimization Techniques for Engineering Design", McGraw-Hill, 1984.

[4] Johnson, Ray C.,"Optimum Design of Mechanical Elements", John Wiley & Sons, 1980.

[5] Savage, M., Coy, J.J., and Townsend, D.P.,"Optimal Tooth Numbers for Compact Standard Spur Gear Sets", Journal of Mechanical Design, Transactions of the ASME, p749-758, October 1982.

[6] Carroll, R.K., and Johnson, G.E.,"Optimal Design of Compact Spur Gear Sets", Journal of Mechanisms, Transmissions, and Automation in Design, Transactions of the ASME, p95-101, March 1984.

[7] Vanderplaats, G.N., Xiang Chen and Ning-Tian Zhang,"Gear Optimization", NASA Contractor Report 4201, NASA Scientific and Technical Information Division, 1988.

[8] Lin, K.C., and Johnson, G.E.,"A Hybrid Expert System - Nonlinear Programming Approach to Optimal Gear Design", Proceedings of the 17^{th} Design Automation Conference, Chicago, 1990.

[9] Muthukrishnan, S.N.,"Computer Aided Optimal Design of Helical Gears", Master's Thesis, Portland State University, 1990.

[10] Shigley, Joseph E., and Mischke, Charles R.,"Standard Handbook of Machine Design", McGraw-Hill, 1986.

[11] "Gleason Bevel & Hypoid Gear Design", Gleason Works, 1956.

[12] Zoutendijk, G.,"Method of Feasible Directions", Elsevier, Amsterdam, 1960.

[13] Yong Chen and Bailin Li,"A Modification of Feasible Direction Optimization Method for Handling Equality Constraints", Journal of Mechanisms, Transmissions, and Automation in Design, Vol. 111, p443-445, 1989.

[14] Press, William H., Flannery, Brian P., Teukolsky, Saul A., and Vetterling, William T., "Numerical Recipes in C: The Art of Scientific Computing", Cambridge University Press, 1988.

[15] Topkis, D.M., and A.F.Veinott,"On the Convergence of Some Feasible Direction Algorithms for Nonlinear Programming", SIAM J. Control, 5, p268-279 (1967).

APPENDIX A

TABLES USED IN HYPOID GEAR DESIGN

MATERIAL FACTORS C_m

Gear		Pinion		Material factor C_M
Material	Hardness	Material	Hardness	
Case-hardened steel	58 R_C†	Case-hardened steel	60 R_C†	0.85‡
Case-hardened steel	55 R_C†	Case-hardened steel	55 R_C†	1.00
Flame-hardened steel	50 R_C†	Case-hardened steel	55 R_C†	1.05
Flame-hardened steel	50 R_C†	Flame-hardened steel	50 R_C†	1.05
Oil-hardened steel	375–425 H_B	Oil-hardened steel	375–425 H_B	1.20
Heat-treated steel	250–300 H_B	Case-hardened steel	55 R_C†	1.45
Heat-treated steel	210–245 H_B	Heat-treated steel	245–280 H_B	1.65
Cast iron		Case-hardened steel	55 R_C†	1.95
Cast iron		Flame-hardened steel	50 R_C†	2.00
Cast iron		Annealed steel	160–200 H_B	2.10
Cast iron		Cast iron		3.10

†Minimum values.
‡Gears must be file-hard.

Source: [10]

RECOMMENDED TOOTH NUMBERS FOR AUTOMOTIVE APPLICATIONS

Approximate ratio	Preferred no. pinion teeth	Allowable range
1.50/1.75	14	12 to 16
1.75/2.00	13	11 to 15
2.0/2.5	11	10 to 13
2.5/3.0	10	9 to 11
3.0/3.5	10	9 to 11
3.5/4.0	10	9 to 11
4.0/4.5	9	8 to 10
4.5/5.0	8	7 to 9
5.0/6.0	7	6 to 8
6.0/7.5	6	5 to 7
7.5/10.0	5	5 to 6

Source: [10]

DEPTH FACTOR

Type of gear	No. pinion teeth	Depth factor k_1
Straight bevel	12 and higher	2.000
Spiral bevel	12 and higher	2.000
	11	1.995
	10	1.975
	9	1.940
	8	1.895
	7	1.835
	6	1.765
Zerol bevel	13 and higher	2.000
Hypoid	11 and higher	4.000
	10	3.900
	9	3.8
	8	3.7
	7	3.6
	6	3.5

Source: [10]

MEAN ADDENDUM FACTOR

Type of gear	No. pinion teeth	Mean addendum factor C_1
Straight bevel	12 and higher	C_1†
Spiral bevel	12 and higher	C_1†
	11	0.490
	10	0.435
	9	0.380
	8	0.325
	7	0.270
	6	0.215
Zerol bevel	13 and higher	C_1†
Hypoid	21 and higher	C_1†
	9 to 20	0.170
	8	0.150
	7	0.130
	6	0.110

†Use $C_1 = 0.270 + 0.230/(m_{90})^2$.

Source: [10]

CLEARANCE FACTORS

Type of gear	Clearance factor k_2
Straight bevel	0.140
Spiral bevel	0.125
Zerol bevel	0.110
Hypoid	0.150

Source: [10]

OVERLOAD FACTORS K_O, C_O

Prime mover	Character of load on driven member		
	Uniform	Medium shock	Heavy shock
Uniform	1.00	1.25	1.75
Medium shock	1.25	1.50	2.00
Heavy shock	1.50	1.75	2.25

†This table is for speed-decreasing drive; for speed-increasing drives add $0.01(N/n)^2$ to the above factors.

Source: [11]

LOAD DISTRIBUTION FACTORS K_m, C_m

Application	Both members straddle-mounted	One member straddle-mounted	Neither member straddle-mounted
General industrial	1.00–1.10	1.10–1.25	1.25–1.40
Automotive	1.00–1.10	1.10–1.25	
Aircraft	1.00–1.25	1.10–1.40	1.25–1.50

Source: [11]

ALLOWABLE CONTACT STRESS, S_{ac}

Material	Heat treatment	Minimum hardness		Contact stress S_{ac}, lb/in^2
		Brinell	Rockwell C	
Steel	Carburized (case-hardened)		60	250 000
Steel	Carburized (case-hardened)		55	210 000
Steel	Flame- or induction-hardened	500	50	200 000
Steel and nodular iron	Hardened and tempered	400		180 000
Steel	Nitrided		60	180 000
Steel and nodular iron	Hardened and tempered	300		140 000
Steel and nodular iron	Hardened and tempered	180		100 000
Cast iron	As cast	200		80 000
Cast iron	As cast	175		70 000
Cast iron	As cast			60 000

Source: [10]

ALLOWABLE BENDING STRESS, S_{at}

Material	Heat treatment	Surface hardness		Bending stress S_{at}, lb/in²
		Brinell	Rockwell C	
Steel	Carburized (case-hardened)	575–625	55 min.	60 000
Steel	Flame- or induction-hardened (unhardened root fillet)	450–500	50 min.	27 000
Steel	Hardened and tempered	450 min.		50 000
Steel	Hardened and tempered	300 min.		42 000
Steel	Hardened and tempered	180 min.		28 000
Steel	Normalized	140 min.		22 000
Cast iron	As cast	200 min.		13 000
Cast iron	As cast	175 min.		8 500
Cast iron	As cast			5 000

Source: [10]

APPENDIX B

GRAPHS USED IN HYPOID GEAR DESIGN

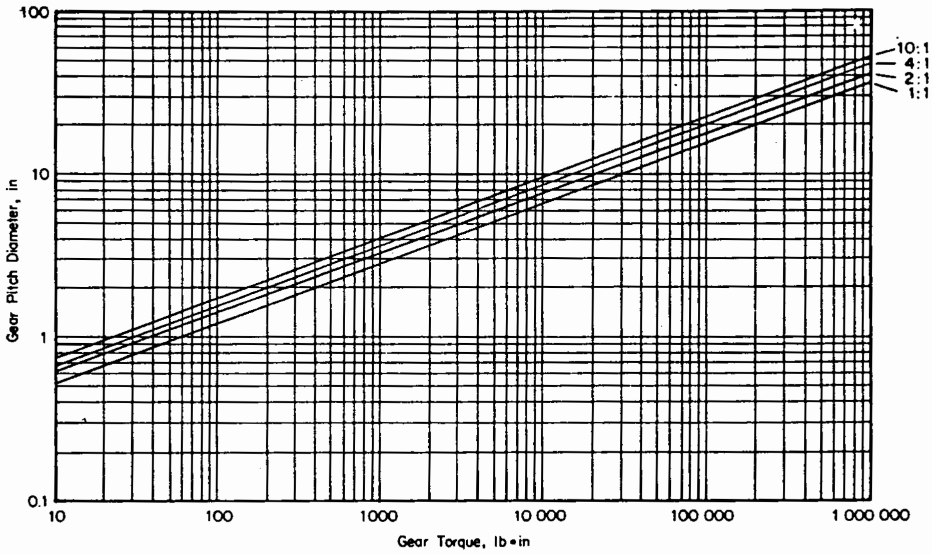

Gear pitch diameter based on surface durability. Source: [10]

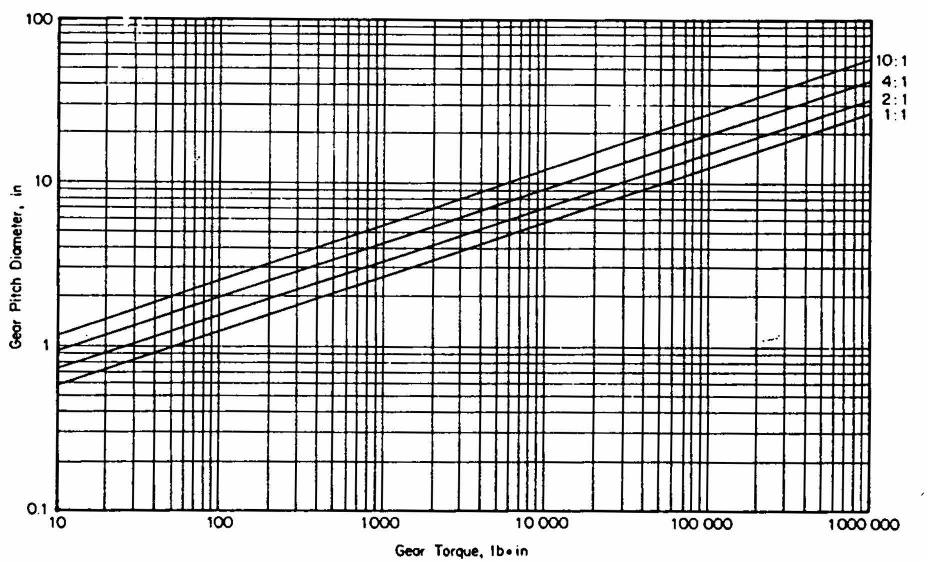

Gear pitch diameter based on bending strength. Source: [10]

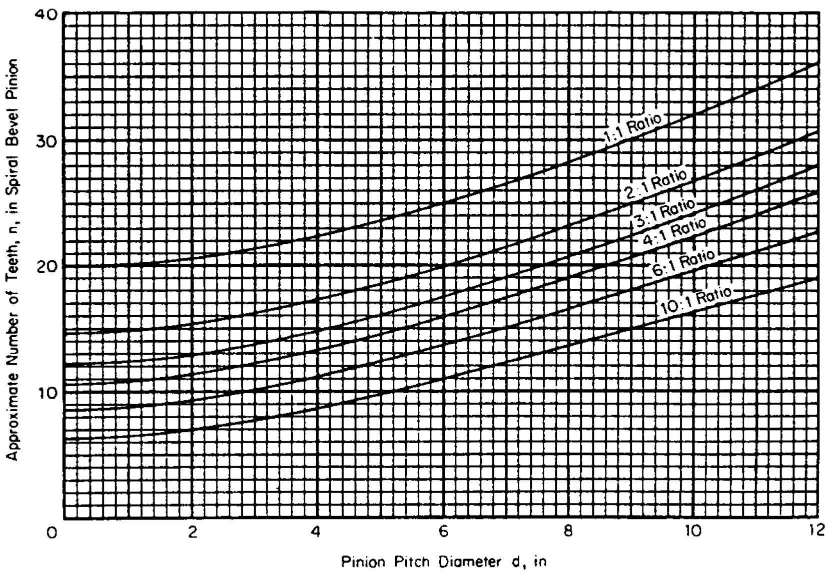

Recommended tooth numbers for hypoid gears. Source: [10]

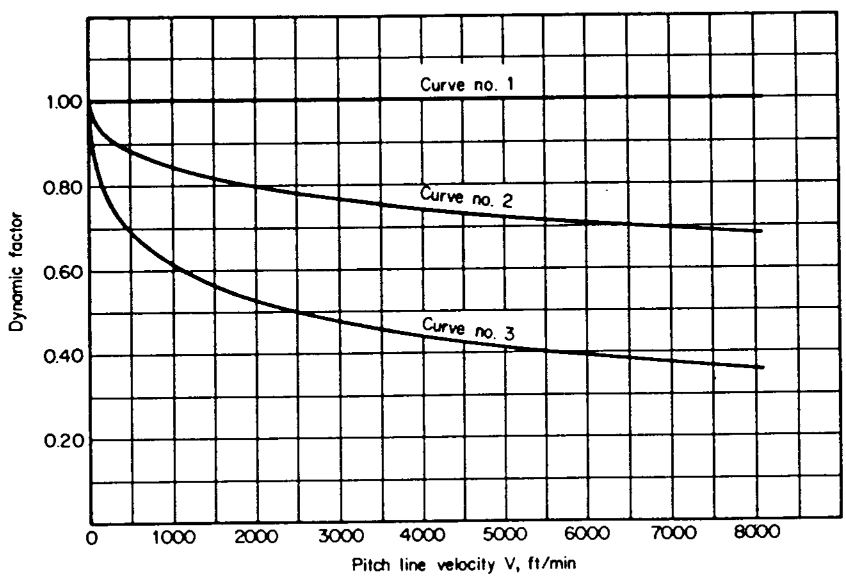

Dynamic factors K_v and C_v. Source: [11]

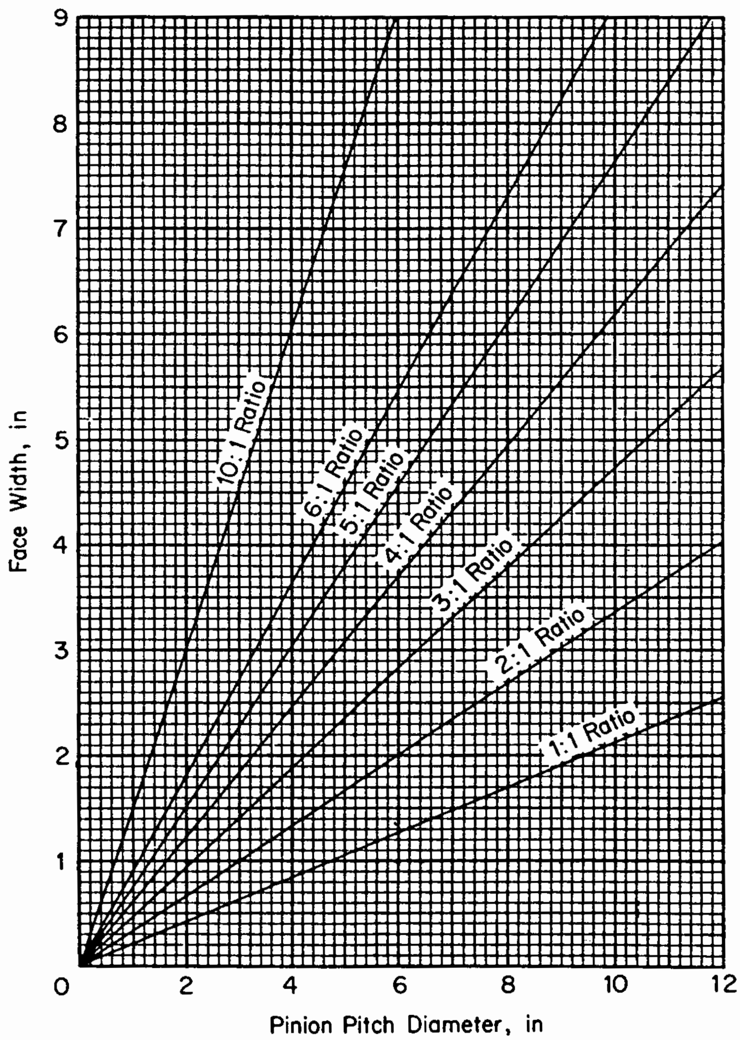

Facewidth of hypoid gears. Source: [11]

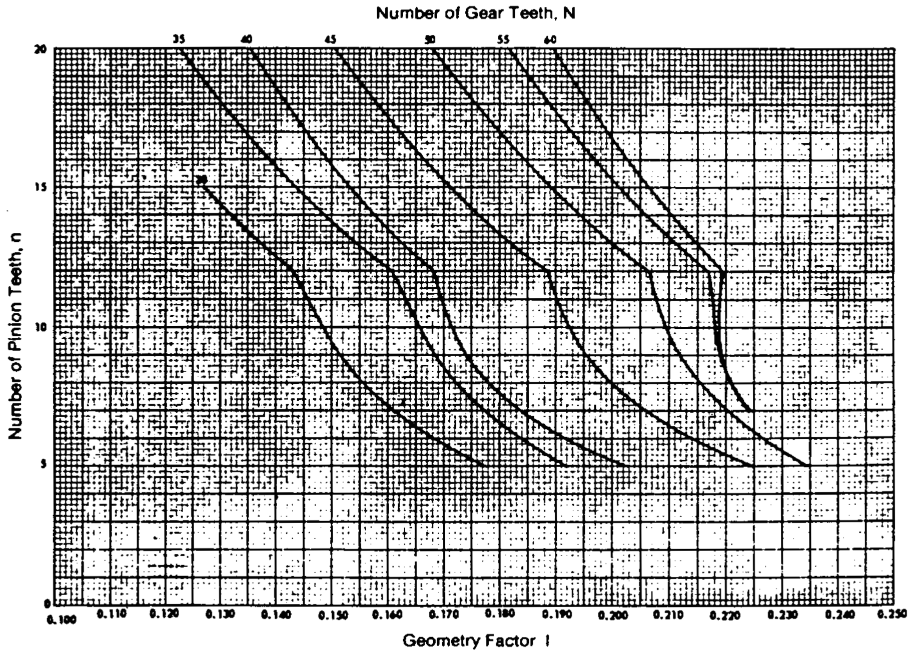

Geometry factor I for durability of hypoid gears with 19° average

pressure angle and E/D ratio of 0.10. Source: [11]

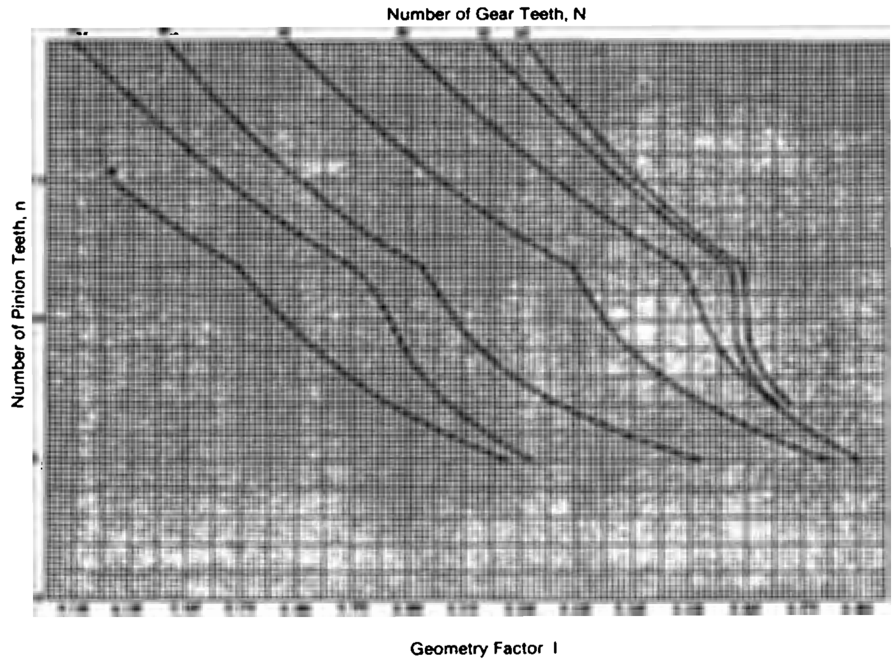

Geometry factor I for durability of hypoid gears with 19°average

pressure angle and E/D ratio of 0.15. Source: [11]

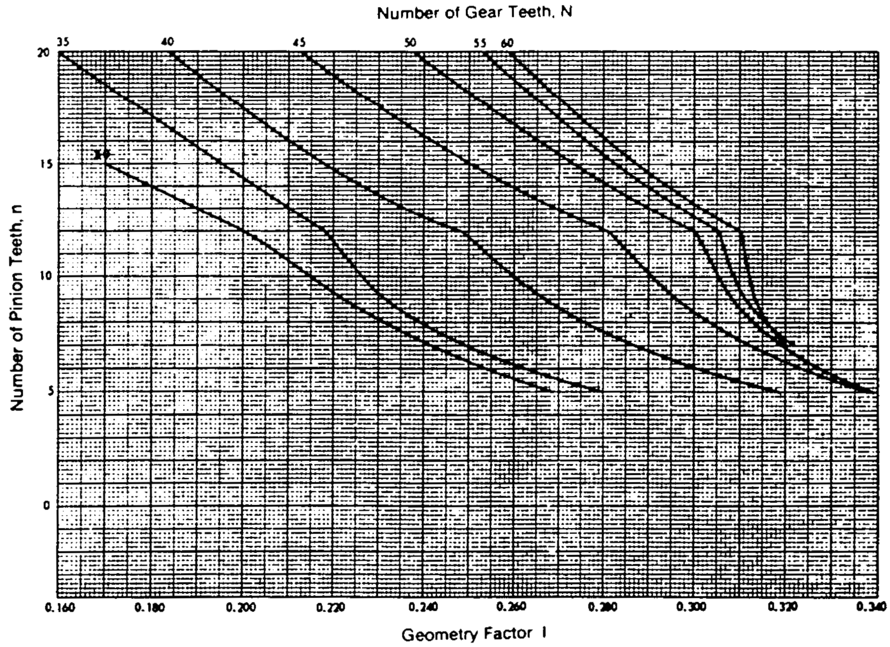

Geometry factor I for durability of hypoid gears with 19° average pressure angle and E/D ratio of 0.20. Source: [11]

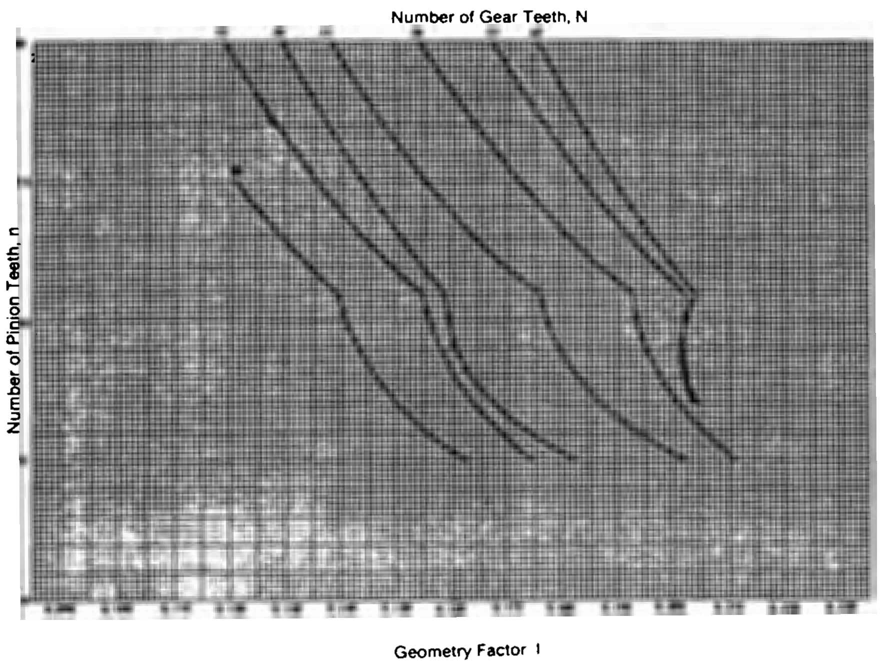

Geometry factor I for durability of hypoid gears with 22.5°average pressure angle and E/D ratio of 0.10. Source: [11]

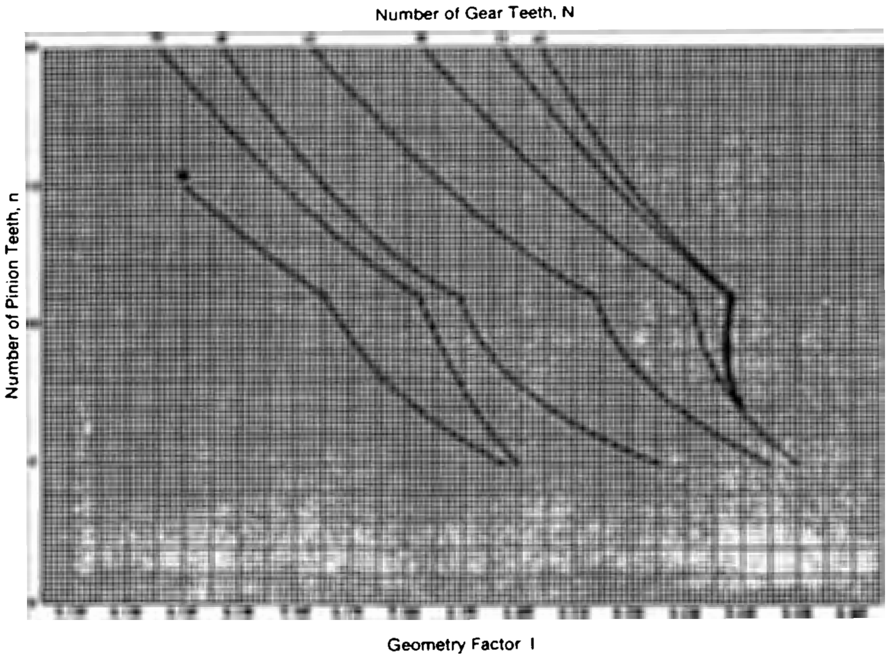

Geometry factor I for durability of hypoid gears with 22.5° average pressure angle and E/D ratio of 0.15. Source: [11]

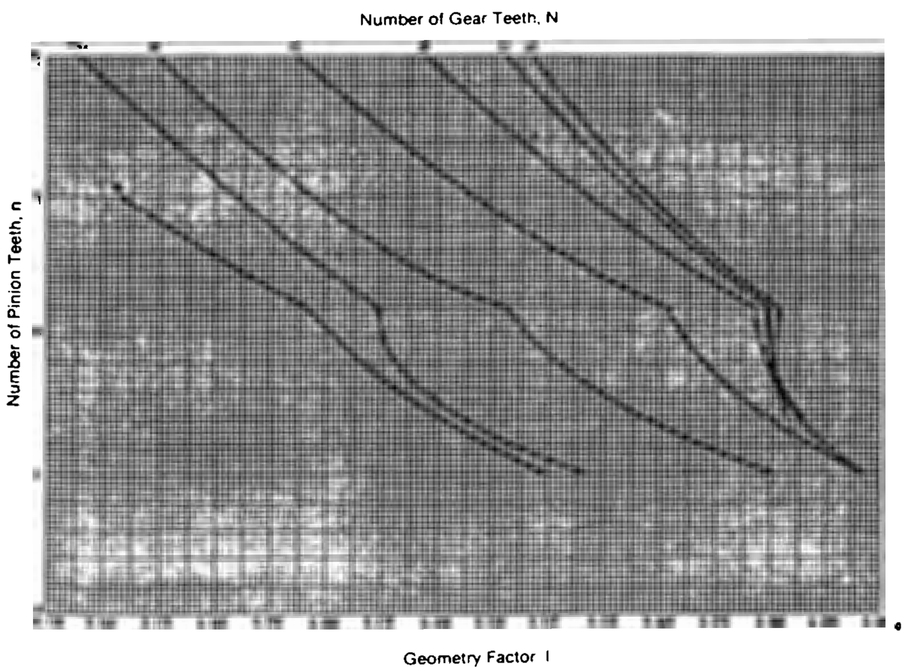

Geometry factor I for durability of hypoid gears with 22.5°average pressure angle and E/D ratio of 0.20. Source: [11]

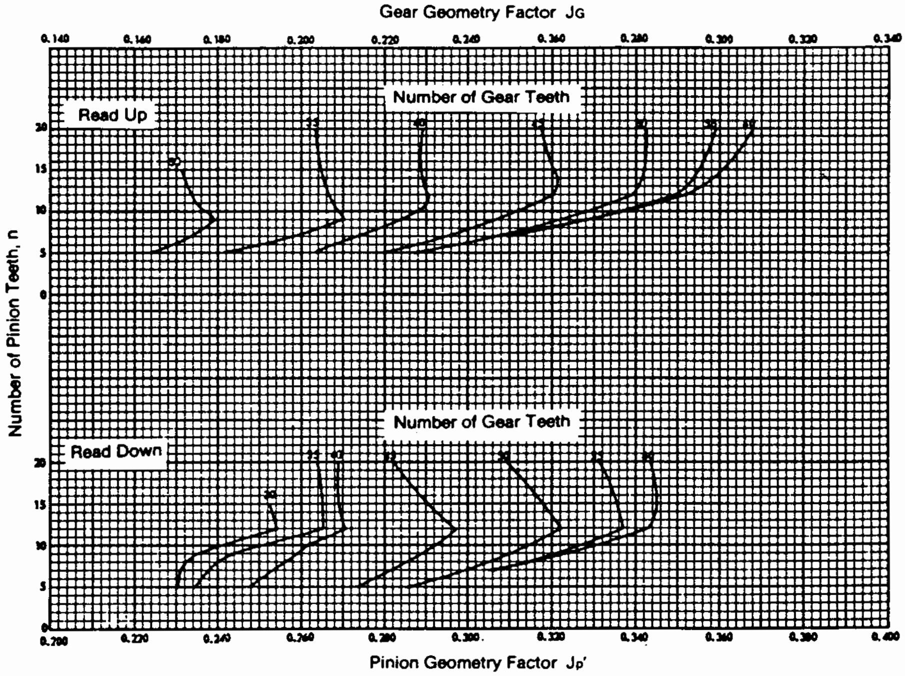

Geometry factor J for strength of hypoid gears with 19° average

pressure angle and E/D ratio of 0.10. Source: [11]

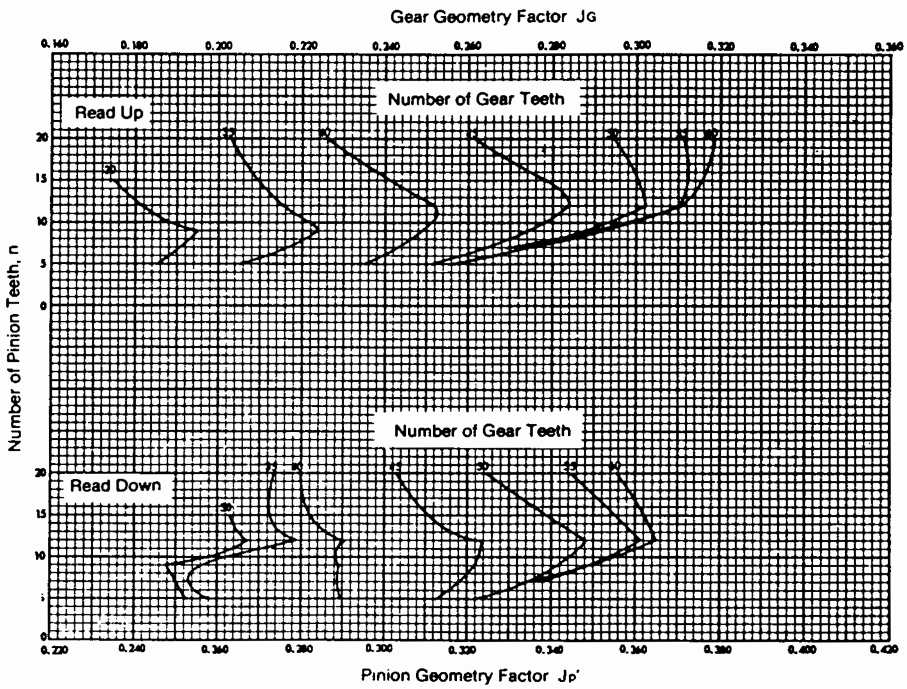

Geometry factor J for strength of hypoid gears with 19° average

pressure angle and E/D ratio of 0.15. Source: [11]

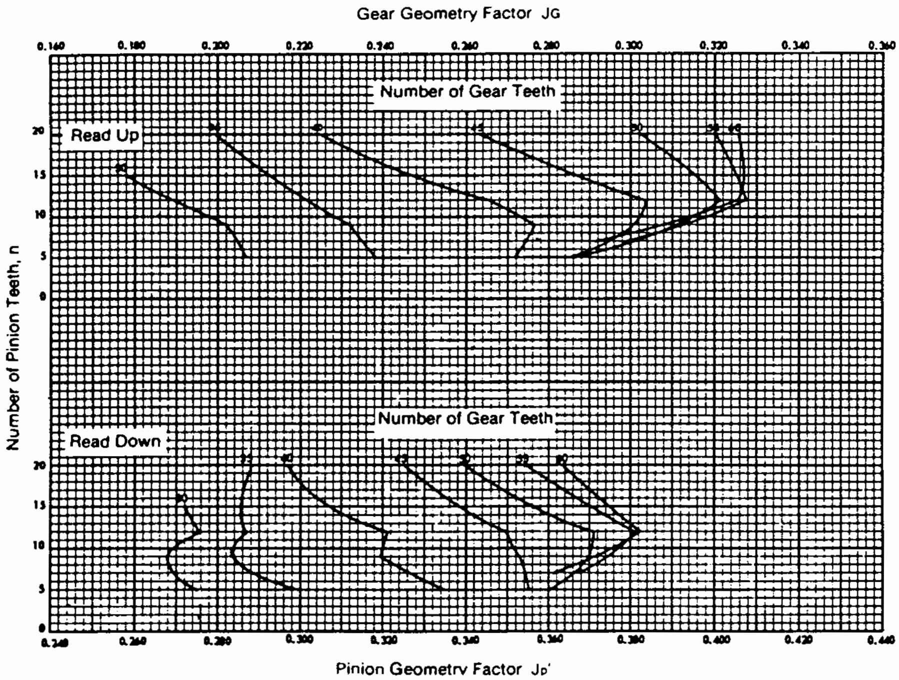

Geometry factor J for strength of hypoid gears with 19° average pressure angle and E/D ratio of 0.20. Source: [11]

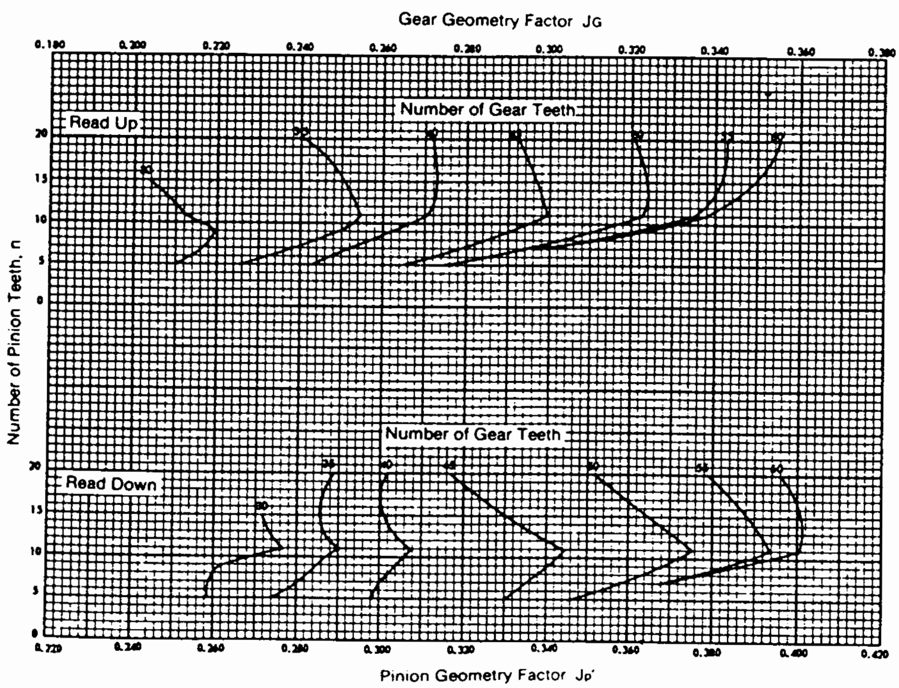

Geometry factor J for strength of hypoid gears with 22.5° average pressure angle and E/D ratio of 0.10. Source: [11]

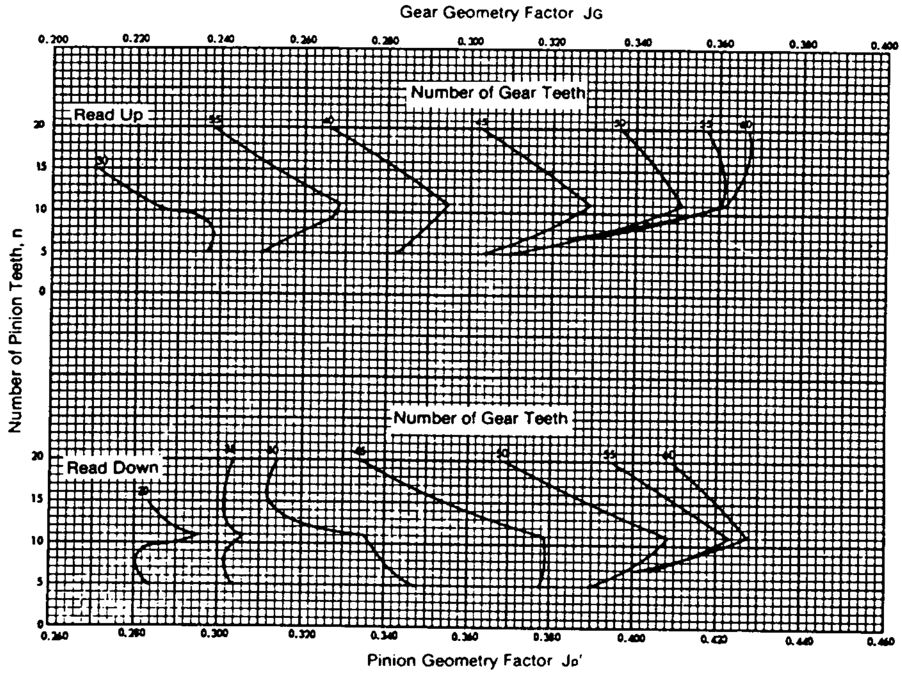

Geometry factor J for strength of hypoid gears with 22.5° average pressure angle and E/D ratio of 0.15. Source: [11]

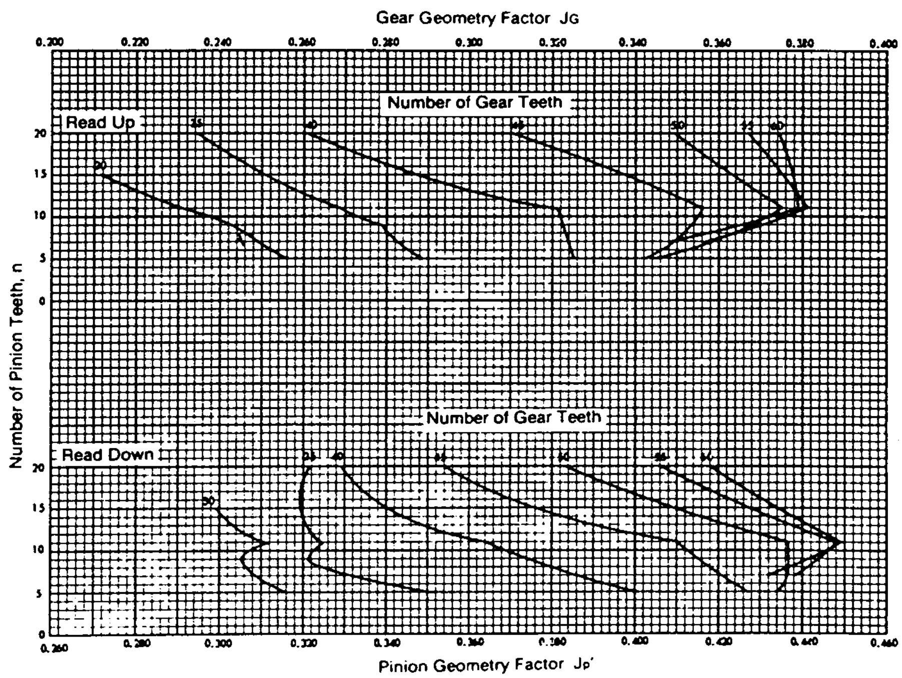

Geometry factor J for strength of hypoid gears with 22.5° average pressure angle and E/D ratio of 0.20. Source: [11]

APPENDIX C

FORMULAS FOR CALCULATING HYPOID DIMENSIONS

FORMULAS FOR COMPUTING BLANK AND TOOTH DIMENSIONS OF HYPOID GEARS

Item	No.	Formula
Pitch diameter of gear	1	$D = \frac{N}{P_d}$
	2	$m = \frac{n}{N}$
	3	$\psi_{Po} = \psi_P$
	4	$\Delta\Sigma = 90 - \Sigma$
	5	$\tan \Gamma_i = \frac{\cos \Delta\Sigma}{1.2(m - \sin \Delta\Sigma)}$
	6	$R = 0.5(D - F \sin \Gamma_i)$
	7	$\sin \varepsilon_i' = \frac{E}{R} \sin \Gamma_i$
	8	$K_1 = \tan \psi_{Po} \sin \varepsilon_i' + \cos \varepsilon_i'$
	9	$R_{P2} = mRK_1$
	10	$\tan \eta = \frac{E}{R(\tan \Gamma_i \cos \Delta\Sigma - \sin \Delta\Sigma) + R_{P2}}$ first trial
	11	$\sin \varepsilon_2 = \frac{E - R_{P2} \sin \eta}{R}$
	12	$\tan \gamma_2 = \frac{\sin \eta}{\tan \varepsilon_2 \cos \Delta\Sigma} + \tan \Delta\Sigma \cos \eta$
	13	$\sin \varepsilon_2' = \frac{\sin \varepsilon_2 \cos \Delta\Sigma}{\cos \gamma_2}$
	14	$\tan \psi_{P2} = \frac{K_1 - \cos \varepsilon_2'}{\sin \varepsilon_2'}$
	15	$\Delta K = \sin \varepsilon_2' (\tan \psi_{Po} - \tan \psi_{P2})$
	16	$\frac{\Delta R_P}{R} = m(\Delta K)$
	17	$\sin \varepsilon_1 = \sin \varepsilon_2 - \frac{\Delta R_P}{R} \sin \eta$
Pinion pitch angle	18	$\tan \gamma = \frac{\sin \eta}{\tan \varepsilon_1 \cos \Delta\Sigma} + \tan \Delta\Sigma \cos \eta$
	19	$\sin \varepsilon_1' = \frac{\sin \varepsilon_1 \cos \Delta\Sigma}{\cos \gamma_1}$
Pinion spiral angle	20	$\tan \psi_P = \frac{K_1 + \Delta K - \cos \varepsilon_1'}{\sin \varepsilon_1'}$

Source: [10]

FORMULAS FOR COMPUTING BLANK AND TOOTH DIMENSIONS OF HYPOID GEARS

(*Continued*)

Item	No.	Formula
Gear spiral angle	21	$\psi_G = \psi_P - \varepsilon_1'$
Gear pitch angle	22	$\tan \Gamma = \dfrac{\sin \varepsilon_1}{\tan \eta \cos \Delta\Sigma} + \cos \varepsilon_1 \tan \Delta\Sigma$
Gear mean cone distance	23	$A_{mG} = \dfrac{R}{\sin \Gamma}$
Pinion mean cone distance	24	$\Delta R_P = R\left(\dfrac{\Delta R_P}{R}\right)$
	25	$A_{mP} = \dfrac{R_{P2} + \Delta R_P}{\sin \gamma}$
	26	$R_P = A_{mP} \sin \gamma$
Limit pressure angle	27	$-\tan \phi_{01} = \dfrac{\tan \gamma \tan \Gamma}{\cos \varepsilon_1'} \times \dfrac{A_{mP} \sin \psi_P - A_{mG} \sin \psi_G}{A_{mP} \tan \gamma + A_{mG} \tan \Gamma}$
	28	$\text{Den} = -\tan \phi_{01}\left(\dfrac{\tan \psi_P}{A_{mP} \tan \gamma} + \dfrac{\tan \psi_G}{A_{mG} \tan \Gamma}\right) + \dfrac{1}{A_{mP} \cos \psi_P} - \dfrac{1}{A_{mG} \cos \psi_G}$
	29	$r_{c1} = \dfrac{\sec \phi_{01} (\tan \psi_P - \tan \phi_G)}{\text{Den}}$
	30	$\left\lvert \dfrac{r_{c*}}{r_{c1}} - 1 \right\rvert \leq 0.01$ Loop back to no. 10 and change η until satisfied.
Gear pitch apex beyond crossing point	31	$Z_P = A_{mP} \tan \gamma \sin \Gamma - \dfrac{E \tan \Delta\Sigma}{\tan \varepsilon_1}$
	32	$Z = \dfrac{R}{\tan \Gamma} - Z_P$
Gear outer cone distance	33	$A_o = \dfrac{0.5D}{\sin \Gamma}$
	34	$\Delta F_o = A_o - A_{mG}$
Depth factor	35	k_1 (see Table 34-5)
Addendum factor	36	C_1 (see Table 34-7)
Mean working depth	37	$h = \dfrac{k_1 R \cos \psi_G}{N}$
Mean addendum	38	$a_P = h - a_G \qquad a_G = C_1 h$

Source: [10]

FORMULAS FOR COMPUTING BLANK AND TOOTH DIMENSIONS OF HYPOID GEARS

(Continued)

Item	No.	Formula
Clearance factor	39	k_2 (see Table 34-6)
Mean dedendum	40	$b_P = b_G + a_G - a_P \quad b_G = h(1 + k_2 - C_1)$
Clearance	41	$c = k_2 h$
Mean whole depth	42	$h_m = a_G + b_G$
Sum of dedendum angle	43	$\Sigma\delta$ (see Sec. 34-5-2)
Gear dedendum angle	44	δ_G (see Sec. 34-5-2)
Gear addendum angle	45	$\alpha_G = \Sigma\delta - \delta_G$
Gear outer addendum	46	$a_{oG} = a_G + \Delta F_o \sin \alpha_G$
Gear outer dedendum	47	$b_{oG} = b_G + \Delta F_o \sin \delta_G$
Gear whole depth	48	$h_t = a_{oG} + b_{oG}$
Gear working depth	49	$h_k = h_{tG} - c$
Gear root angle	50	$\Gamma_R = \Gamma - \delta_G$
Gear face angle	51	$\Gamma_o = \Gamma + \alpha_G$
Gear outside diameter	52	$D_o = 2a_{oG} \cos \Gamma + D_G$
Gear crown to crossing point	53	$X_o = Z_P + \Delta F_o \cos \Gamma - a_{oG} \sin \Gamma$
Gear root apex beyond crossing point	54	$Z_R = Z + \dfrac{A_{mG} \sin \delta_G - b_G}{\sin \Gamma_R}$
Gear face apex beyond crossing point	55	$Z_o = Z + \dfrac{A_{mG} \sin \alpha_G - a_G}{\sin \Gamma_o}$
	56	$Q_R = \dfrac{A_{mG} \cos \delta_G}{\cos \Gamma_R} - Z$
	57	$Q_o = \dfrac{A_{mG} \cos \alpha_G}{\cos \Gamma_o} - Z$
	58	$\tan \xi_R = \dfrac{E \tan \Delta\Sigma}{Q_R}$

Source: [10]

FORMULAS FOR COMPUTING BLANK AND TOOTH DIMENSIONS OF HYPOID GEARS

(Continued)

Item	No.	Formula
Gear face apex beyond crossing point (*continued*)	59	$\tan \xi_o = \dfrac{E \tan \Delta\Sigma}{Q_o}$
	60	$\sin(\varepsilon_R + \xi_R) = \dfrac{E \cos \xi_R \tan \Gamma_R}{Q_R}$
	61	$\sin(\varepsilon_o + \xi_o) = \dfrac{E \cos \xi_o \tan \Gamma_o}{Q_o}$
Pinion face angle	62	$\sin \gamma_o = \sin \Delta\Sigma \sin \Gamma_R + \cos \Delta\Sigma \cos \Gamma_R \cos \varepsilon_R$
Pinion root angle	63	$\sin \gamma_R = \sin \Delta\Sigma \sin \Gamma_o + \cos \Delta\Sigma \cos \Gamma_o \cos \varepsilon_o$
Pinion face apex beyond crossing point	64	$G_o = \dfrac{E \sin \varepsilon_R \cos \Gamma_R - Z_R \sin \Gamma_R - c}{\sin \gamma_o}$
Pinion root apex beyond crossing point	65	$G_R = \dfrac{E \sin \varepsilon_o \cos \Gamma_o - Z_o \sin \Gamma_o - c}{\sin \gamma_R}$
	66	$\tan \lambda' = \dfrac{m \sin \varepsilon_i' \cos \Gamma}{\cos \gamma + m \cos \Gamma \cos \varepsilon_i'}$
Pinion addendum angle	67	$\alpha_P = \gamma_o - \gamma$
Pinion dedendum angle	68	$\delta_P = \gamma - \gamma_R$
Pinion whole depth	69	$h_{tP} = \dfrac{(x_o + G_o) \sin \delta_P}{\cos \gamma_o} - \sin \gamma_R (G_R - G_o)$
	70	$\Delta F_i = F - \Delta F_o$
	71	$\Delta F_{oP} = h \sin \varepsilon_R (1 - m)$
	72	$F_{oP} = \dfrac{\Delta F_o \cos \lambda'}{\cos(\varepsilon_i' - \lambda')}$
	73	$F_{iP} = \dfrac{\Delta F_i \cos \lambda'}{\cos(\varepsilon_i' - \lambda')}$
	74	$\Delta B_o = \dfrac{F_o \cos \gamma_o}{\cos \alpha_P} + \Delta F_{oP} - (b_G - c) \sin \gamma$
	75	$\Delta B_i = \dfrac{F \cos \gamma_o}{\cos \alpha_P} + \Delta F_{oP} - (b_G - c) \sin \gamma$
Pinion crown to crossing point	76	$x_o = \dfrac{E}{\tan \varepsilon_1 \cos \Delta\Sigma} - R_P \tan \gamma + \Delta B_o$

Source: [10]

FORMULAS FOR COMPUTING BLANK AND TOOTH DIMENSIONS OF HYPOID GEARS

(Continued)

Item	No.	Formula
Pinion front crown to crossing point	77	$x_i = \dfrac{E}{\tan \epsilon_1 \cos \Delta\Sigma} - R_P \tan \gamma - \Delta B_i$
Pinion outside diameter	78	$d_o = 2 \tan \gamma_o (x_o + G_o)$
Pinion face width	79	$F_P = \dfrac{x_o - x_i}{\cos \gamma_o}$
Mean circular pitch	80	$p_m = \dfrac{\pi A_{mG}}{P_d A_o}$
Mean diametral pitch	81	$P_{dm} = P_d \dfrac{A_o}{A_{mG}}$
Thickness factor	82	K (see Fig. 34-17)
Mean pitch diameter	83	$d_m = 2A_{mP} \sin \gamma$
	84	$D_m = 2A_{mG} \sin \Gamma$
Mean normal circular thickness	85	$t_n = p_m \cos \psi_G - T_n$
	86	$T_n = 0.5p_m \cos \psi_G - (a_P - a_G) \tan \phi + \dfrac{K \cos \psi}{P_{dm} \tan \phi}$
Outer normal backlash allowance	87	B (see Table 34-8)
Mean normal chordal thickness	88	$t_{nc} = t_n - \dfrac{t_n^3}{6d_m^2} - 0.5B \sec \phi \left(\dfrac{A_{mg}}{A_o}\right)$
	89	$T_{nc} = T_n - \dfrac{T_n^3}{6D_m^2} - 0.5B \sec \phi \left(\dfrac{A_{mG}}{A_o}\right)$
Mean chordal addendum	90	$a_{cP} = a_P + \dfrac{0.25t_n^2 \cos \gamma}{d_m}$
	91	$a_{cG} = a_G + \dfrac{0.25T_N^2 \cos \Gamma}{D_m}$

Source: [10]

APPENDIX D

EXAMPLE OF GRAPH CONVERSION TO POLYNOMIAL EQUATIONS

POLYNOMIAL COEFFICIENTS

Degree	Order 6	Order 7	Order 8	Order 9	Order 10
0	-0.148178	-0.966867	2.86164	11.7518	-13.2241
1	0.287798	0.861058	-2.19612	-10.1535	14.5665
2	-0.0782765	-0.242974	0.786377	3.85314	-6.85763
3	0.0104111	0.0356279	-0.155493	-0.824045	1.8532
4	-0.000719314	-0.00294733	0.0184925	0.109454	-0.318452
5	0.0000248185	0.000138748	-0.00135222	-0.0093735	0.0363687
6	0.000000338149	-0.00000346941	0.000059432	0.000518583	-0.00279708
7		0.000000035786	-0.00000143925	-0.0000179161	0.000143193
8			0.00000001475	0.000000351633	-0.00000467644
9				-0.00000000299	0.000000088125
10					-0.00000000073

The above table shows the polynomial coefficients for the geometry factor graph shown in page 59, with 19° average pressure angle and E/D ratio of 0.15. The polynomial coefficients shown above are found for the pinion geometry factor J_p' with the number of gear teeth held constant at 35. This graph was selected as an example to show the accuracy obtained in polynomial conversion. The order of the polynomial coefficients was changed from 6 to 10, to get the best curve fitting. The figures in the following pages show the original curve and the fitted curve for the order 6 to 10. After inspecting each one of them, the order 10 was selected as the best curve fit and used for interpolation. The order 9 which gives a good approximation for higher values of n, i.e. between 15 to 20, does not give as good a value for the lower range of n, i.e. 5 to 10. Since the overall accuracy obtained for order 10 was better it is chosen as the best fit. In the same way polynomial coefficients are found for all the other graphs.

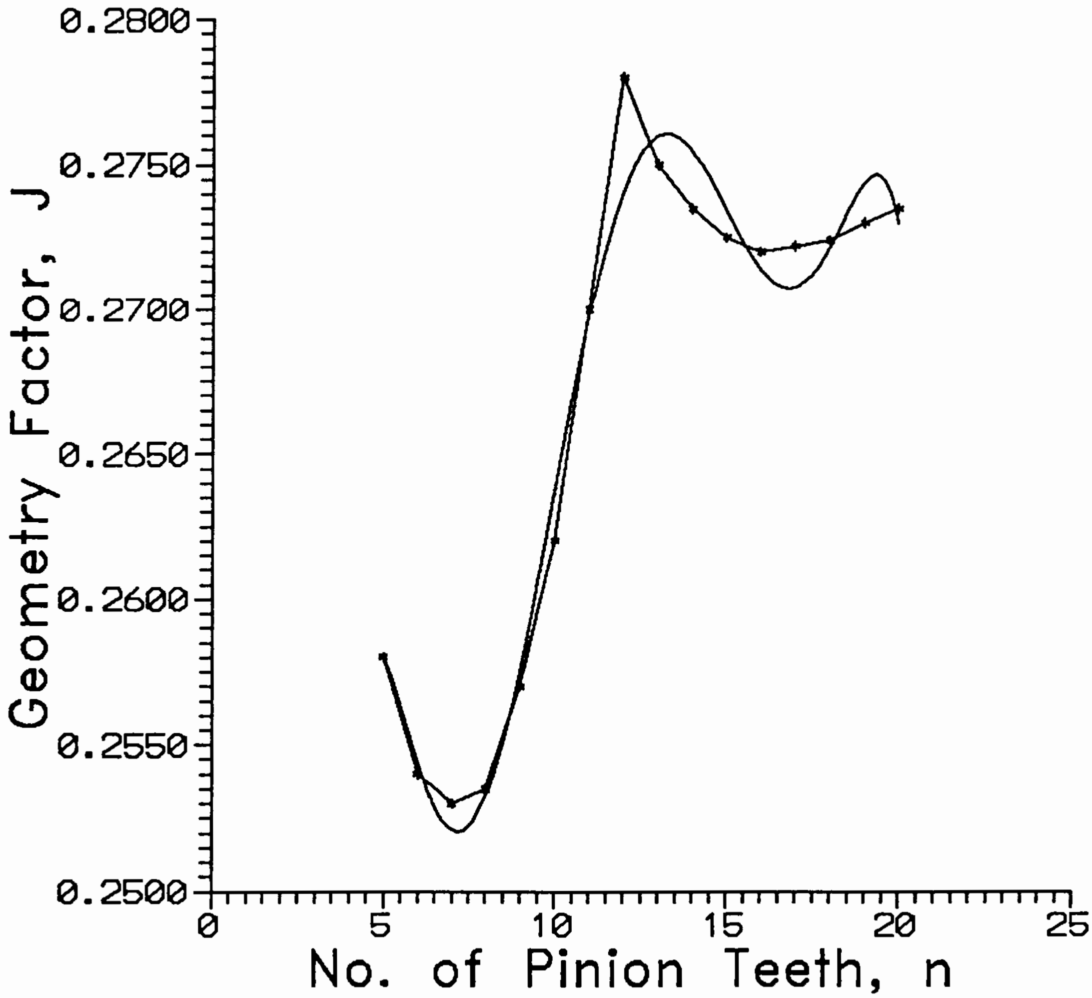

Curve fitting using 6th order polynomial

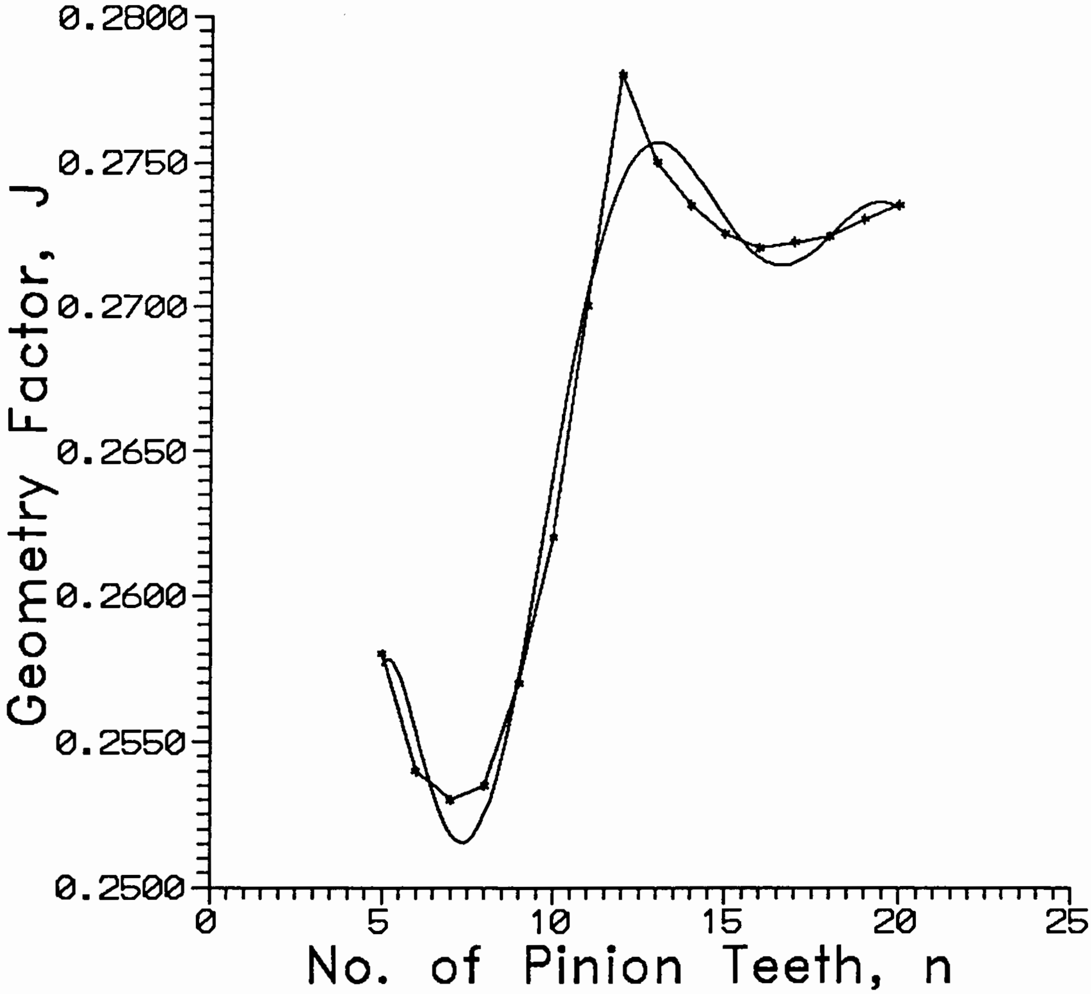

Curve fitting using 7th order polynomial

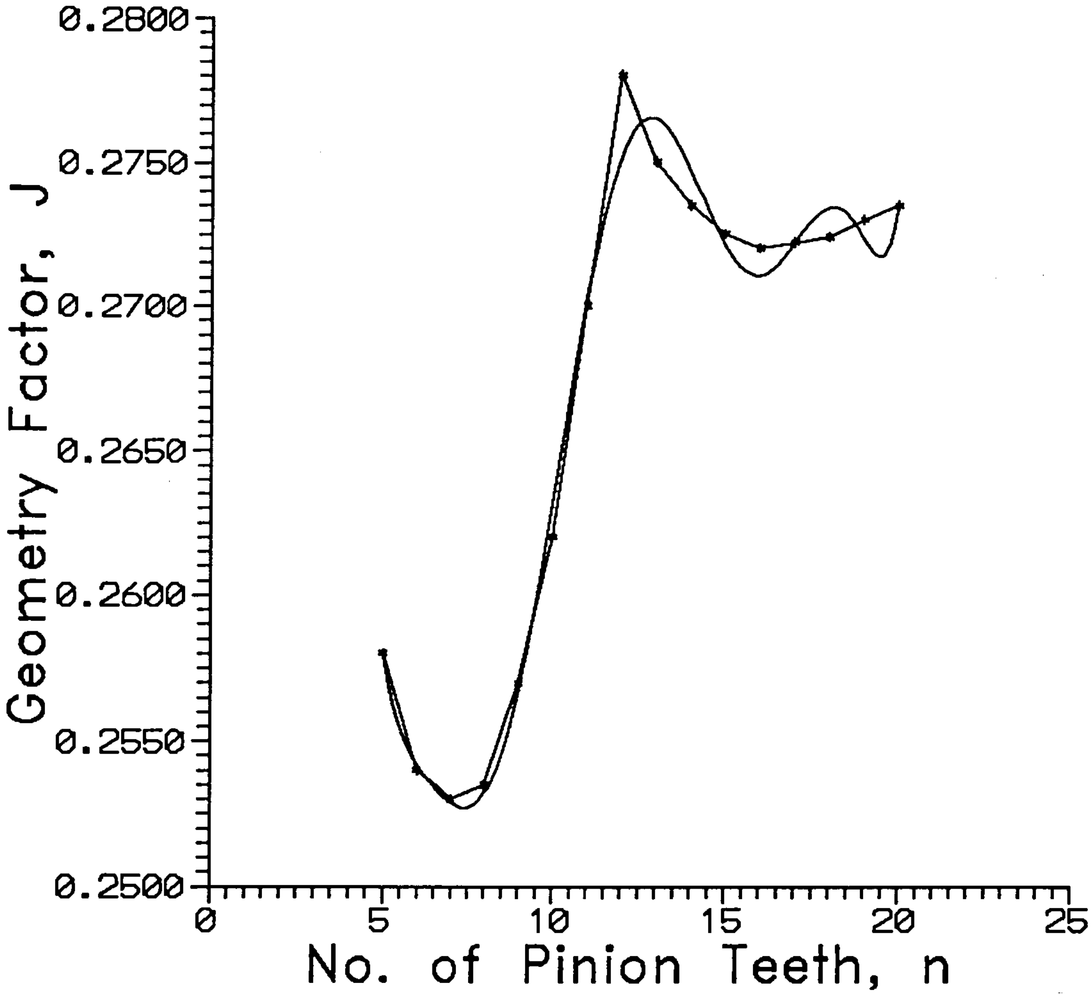

Curve fitting using 8th order polynomial

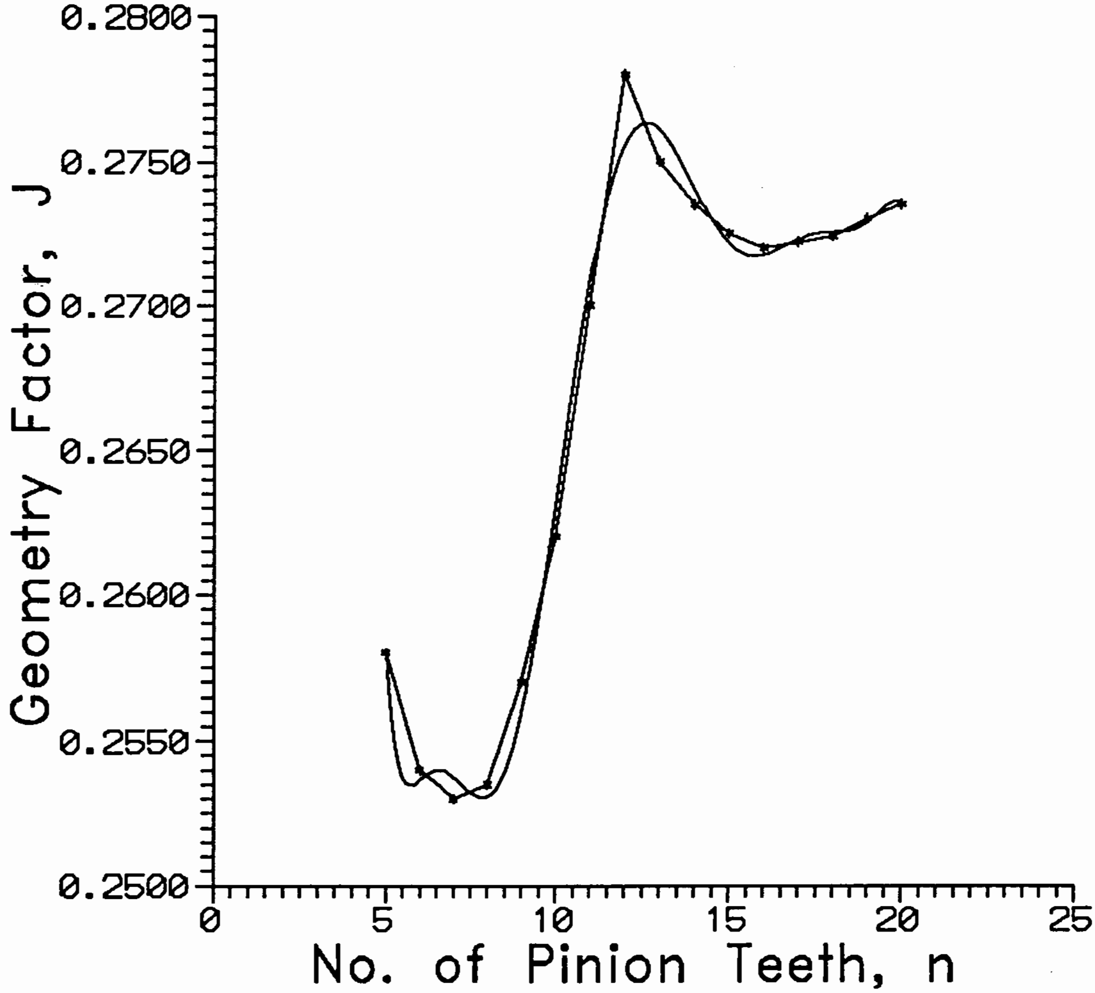

Curve fitting using 9[th] order polynomial

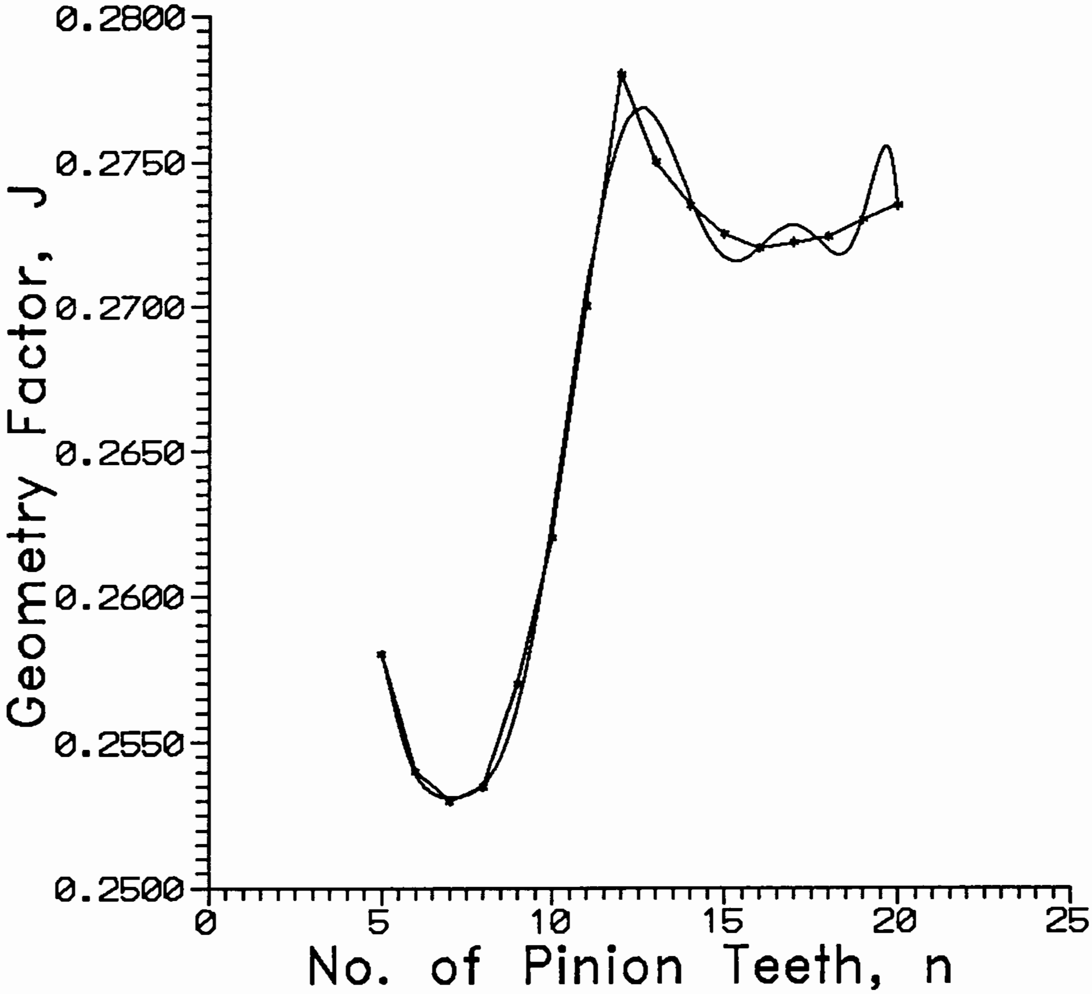

Curve fitting using 10^{th} order polynomial